TAMPERE UNIVERSITY OF TECHNOLOGY

ESA NIEMI

ACOUSTIC OBSTACLE SCATTERING AND THE FACTORIZATION METHOD

Master of Science Thesis

Examiners: Prof. Mikko Kaasalainen,
Prof. Samuli Siltanen
Examiners and topic approved in the
Science and Environmental Engineering
Faculty Council meeting
on 5 May 2010

ABSTRACT

TAMPERE UNIVERSITY OF TECHNOLOGY
Master's Degree Programme in Science and Engineering
ESA NIEMI : Acoustic Obstacle Scattering and the Factorization Method
Master of Science Thesis, 54 pages
June 2010
Major: Mathematics
Examiners: Prof. Mikko Kaasalainen and Prof. Samuli Siltanen
Keywords: acoustic obstacle scattering, inverse scattering, factorization method

Scattering is a physical phenomenon which can be modeled with a boundary value problem for a partial differential equation. This boundary value problem gives rise to two kind of problems: direct scattering problem and inverse scattering problem. In the former one tries to find the solution of the boundary value problem while in the latter the aim is to determine the boundary (of the scatterer) given information about the solution of the boundary value problem. The main goal of this thesis is to analyze the direct scattering problem to an extent that is necessary in order to study the inverse scattering problem both theoretically and numerically.

This thesis establishes that the boundary value problem arising from two-dimensional acoustic obstacle scattering of time-harmonic plane waves has a unique solution. In particular, the so-called far field pattern for the solution is derived; the far field pattern is a central concept in view of the corresponding inverse problem. The inverse problem is briefly considered together with the factorization method for solving the inverse problem. Computational methods both for solving the direct problem and the inverse problem are developed and illustrated with numerical examples.

TIIVISTELMÄ

TAMPEREEN TEKNILLINEN YLIOPISTO
Teknis-luonnontieteellinen koulutusohjelma
ESA NIEMI: Akustinen obstaakkelisironta ja faktorisaatiomenetelmä
Diplomityö, 54 sivua
Kesäkuu 2010
Pääaine: Matematiikka
Tarkastajat: prof. Mikko Kaasalainen ja prof. Samuli Siltanen
Avainsanat: akustinen obstaakkelisironta, käänteinen sironta, inversiosironta, faktorisaatiomenetelmä

Sironta on fysikaalinen ilmiö, jota voidaan mallintaa osittaisdifferentiaaliyhtälön reuna-arvo-ongelmalla. Tähän reuna-arvo-ongelmaan pohjautuu sekä suora että käänteinen sirontaongelma. Suorassa sirontaongelmassa etsitään ratkaisua reuna-arvo-ongelmaan kun taas käänteisessä sirontaongelmassa tavoitteena on määrätä (sirottajan) reuna kun reuna-arvo-ongelman ratkaisu tunnetaan kaukana sirottajasta. Tämän diplomityön päätavoitteena on analysoida suoraa sirontaongelmaa siinä määrin kuin on vastaavaan käänteiseen ongelmaan perehtymisen kannalta tarpeellista.

Tässä diplomityössä tarkastellaan aika-harmonisten akustisten tasoaaltojen kaksiulotteista obstaakkelisirontaa. Erityisesti näytetään että kyseistä suoraa sirontaongelmaa mallintavalla reuna-arvo-ongelmalla on yksikäsitteinen ratkaisu ja johdetaan sille niin kutsuttu kaukokenttäkuvio, joka on keskeinen käsite vastaavan käänteisen ongelman kannalta. Vastaavaa käänteistä ongelmaa ja faktorisaatiomenetelmää sen ratkaisemiseksi tarkastellaan lyhyesti. Lisäksi kehitetään ja havainnollistetaan numeerisin esimerkein laskennallisia menetelmiä sekä suoran että käänteisen ongelman ratkaisemista varten.

PREFACE

This thesis was carried out at the Department of Mathematics, Tampere University of Technology, and at the Department of Mathematics and Statistics, University of Helsinki. The work was supported in part by Academy of Finland, under the grants Research programme on computational science CSI Speech 134868 and Centre of Excellence in Inverse Problems Research 213476.

I would like to thank my supervisor Professor Samuli Siltanen for introducing me to the field of inverse problems and for providing a challenging topic. I also thank him for his helpful guidance and encouragement during the work. Professor Mikko Kaasalainen deserves my thanks for examining this thesis together with Siltanen.

Finally I thank my brother Jari for reading and commenting the manuscript and for stimulating my interest in mathematics during all the years. There are, of course, also many other people who have directly or indirectly contributed to this work, so I express my gratitude to them as well.

Kangasala, May 2010

Esa Niemi

CONTENTS

MATHEMATICAL NOTATION

$\mathbb{R}^n$	n-dimensional Euclidean space
$x \cdot y$	Euclidean inner product of vectors x and y
$\|x\|$	Euclidean norm of vector x
$\overline{\Omega}$	closure of set Ω
$\partial\Omega$	boundary of set Ω
$C(\Omega)$	set of continuous functions on Ω
$C^k(\Omega)$	set of k times continuously differentiable functions on Ω
$L^2(\Omega)$	set of square-integrable functions on Ω
$\bar{z}$	complex conjugate of number $z \in \mathbb{C}$
$\|f\|_{\infty,\Omega} = \|f\|_\infty$	supremum norm of function $f : \Omega \to \mathbb{C}$
S^1	unit circle $\{x \in \mathbb{R}^2 \ : \ \|x\| = 1\}$

1. INTRODUCTION

Acoustic wave motion in homogeneous inviscid fluid propagates "unchangingly" until it encounters an obstacle. Then the incident wave undergoes reflections, that is, the wave is forced to deviate from a straight trajectory. This phenomenon is called scattering, and the wave field caused by reflections is known as scattered field. Figure 1.1 illustrates these concepts.

An interesting question arises: given an incident field and the corresponding scattered field at a large distance from the unknown obstacle, is it possible to determine the shape of the obstacle and if so, how to find the shape? In order to answer this question, several concepts and tools both from physics and mathematics are necessary. This thesis is concerned with the mathematical ones and therefore the starting point is the physical model of acoustic obstacle scattering written in mathematical form.

Because of the large number of different kind of scattering problems, it is not possible to discuss all of them in one thesis. Therefore this work was restricted to consider the case of

(i) two spatial dimensions,

(ii) time-harmonic acoustic plane waves, and

(iii) impenetrable sound-hard obstacles.

Omitting all the details, which will be discussed in Chapter 2, the formulation of the physical scattering model in the case of (i)–(iii) leads to the exterior boundary value problem

$$\begin{aligned} \Delta w(x) + k^2 w(x) &= 0, && x \in \mathbb{R}^2 \setminus \overline{D}, \\ \frac{\partial w}{\partial \nu}(x) &= g(x), && x \in \partial D, \\ \lim_{r\to\infty} \sqrt{r}\left(\frac{\partial w}{\partial r} - ikw\right) &= 0, && r = |x|, \end{aligned} \tag{1.1}$$

where the mapping $w : \mathbb{R}^2 \setminus \overline{D} \to \mathbb{C}$ represents the scattered field, the function g is defined by $g(x) = -(\partial/\partial\nu)e^{ikd\cdot x}$, the set $D \subset \mathbb{R}^2$ depicts an obstacle with a sufficiently smooth boundary ∂D, the vector $\nu = \nu(x)$ denotes the outward unit

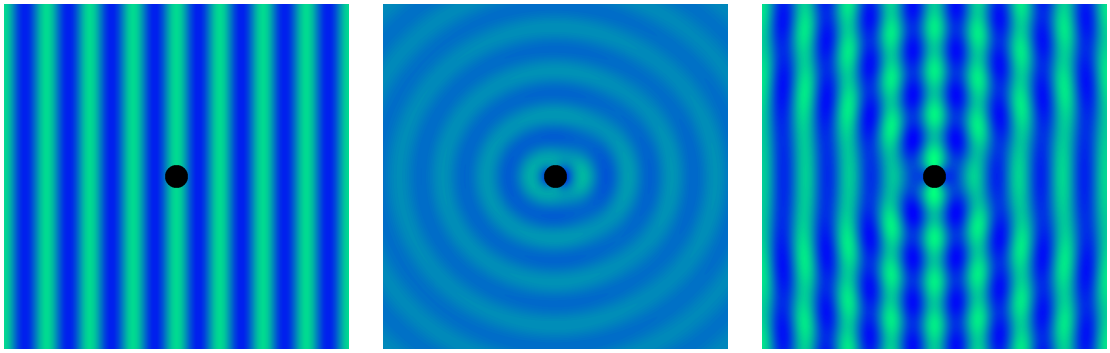

(a) Incident field (plane wave). (b) Scattered field. (c) Total field.

Figure 1.1: Illustration of incident, scattered and total fields. Total field is the sum of incident and scattered fields. The black disks depict the obstacle.

normal to ∂D at $x \in \partial D$, and $k > 0$ and $d \in S^1$ are the wave number and the direction of propagation of the incident plane wave, respectively.

The basic problem regarding the boundary value problem (1.1) is to answer to the questions of uniqueness and existence of solution w, and to find a solution if it exists. This problem is known as the *direct* scattering problem, and physically it corresponds to the problem of determining the scattered field w for a given incident field and obstacle.

A more interesting problem, both from practical and mathematical point of view, is the corresponding *inverse* problem, in which the aim is to find information about the obstacle $D \subset \mathbb{R}^2$ given the incident field and the scattered field at a large distance from the obstacle. The solution of this problem provides an answer to the question addressed in the beginning of this chapter hence being of great interest in terms of applications such as medical imaging, material science, radar, sonar, and nondestructive testing.

This thesis considers both the direct and inverse problem. In terms of the direct problem the uniqueness and existence of its solution are established. The existence proof is based on the method of boundary integral equations and provides us the solution in a form that can be used in numerical computations. The inverse problem is not treated as thoroughly but the uniqueness of its solution is established as well.

The main motivation of this work is twofold. First, despite the fact that most of this thesis is devoted to studying the direct scattering problem, the work aims at studying the inverse scattering problem. It is essential to understand the direct problem in order to understand the inverse problem, since the solution of the inverse problem is also based on the model of the direct problem. The second goal is to develop numerical methods for solving direct scattering problems. These methods can then be used to generate test data for testing the inversion methods computationally.

In addition to the analysis of direct and inverse problems, a relatively new and

promising method, known as factorization method, for solving the inverse problem is studied both theoretically and numerically. The motivation is to demonstrate an approach to the inverse scattering problem and illustrate its numerical performance as well as to verify the computational methods developed for the direct problem.

The standard modern monograph on inverse scattering problems is [5] by David Colton and Rainer Kress. Also their earlier monograph [4] is essential in order to get a thorough analysis of direct scattering problems. The analysis in these monographs is carried out in three dimensions as opposed to the two-dimensional case treated in this thesis. Although the analysis is quite similar in two and three dimensions, there are some differences. The direct problem in two dimensions is treated for example in [13], and two-dimensional inverse scattering problems are considered for example in [2] and [3]. A more explanatory treatment on inverse scattering can be found in [7], where most proofs are omitted but a large number of appropriate references is given.

The factorization method was developed by Andreas Kirsch and Natalia Grinberg in four publications between 1998 to 2004. In 2008 they published a monograph [9] on the method. This monograph presents the theoretical basis of the method and applications to inverse scattering problems and to electrical impedance tomography.

The structure of this thesis is as follows. Chapter 2 is the core of this work. It presents the theory of acoustic obstacle scattering ranging from the physical background of the problem to the uniqueness and existence of its solution. In addition, it introduces the concept of far field pattern which is of central importance in terms of the inverse scattering problem. Chapter 3 briefly discusses the inverse scattering problem, establishes the uniqueness of its solution, and studies the factorization method. Chapter 4 deals with computational methods for solving direct scattering problems as well as a computational implementation of the factorization method. Finally, Chapter 5 presents the numerical results obtained by using the methods developed in Chapter 4, and Chapter 6 is devoted to conclusions.

2. DIRECT ACOUSTIC OBSTACLE SCATTERING PROBLEM

This chapter is devoted to analyzing the boundary value problem arising from acoustic scattering. We begin with a brief discussion on the physical background of the problem. After that we recall some preliminary results needed in the analysis. Then, in the next two sections we establish uniqueness and existence of the solution of the boundary value problem. The existence proof is based on boundary integral equation method and provides us the solution as a single-layer potential representation that can be used to compute the solution numerically. Finally, in the last section we introduce the concept of far field pattern which is of great importance in terms of the inverse scattering problem.

2.1 Physical background

This section deals with the physical background of acoustic obstacle scattering problem in two spatial dimensions. The goal is to explain how the boundary value problem for acoustic obstacle scattering of time-harmonic plane waves is obtained.

Acoustic wave motion in homogeneous isotropic inviscid fluid can be modeled with the partial differential equation

$$\Delta W - \frac{1}{c^2}\frac{\partial^2 W}{\partial t^2} = 0, \tag{2.1}$$

where W is a scalar valued function modeling the wave (field), and c is the speed of sound in the fluid. This is a wave equation that can be derived from more fundamental equations of fluid dynamics, see [5], [8], or [9] for details. In two spatial dimensions (2.1) can be written in the form

$$\frac{\partial^2 W}{\partial {x_1}^2} + \frac{\partial^2 W}{\partial {x_2}^2} - \frac{1}{c^2}\frac{\partial^2 W}{\partial t^2} = 0. \tag{2.2}$$

Physically W corresponds to the velocity potential, that is, the flow velocity of the fluid is given by the gradient of W.

We will consider only time-harmonic waves, so using the convenient way of writing

waves in the complex form, W can be represented as

$$W(x_1, x_2, t) = \mathrm{Re}\left\{w(x_1, x_2)e^{-i\omega t}\right\}, \tag{2.3}$$

where $w : \mathbb{R}^2 \to \mathbb{C}$ is the space dependent part, ω is the angular frequency of the wave motion, and t denotes time. Since the operation of taking the real part commutes with differentiation, the solution of (2.2) can be sought in the complex form $w(x_1, x_2)e^{-i\omega t}$. Substituting this expression into (2.2) yields

$$\frac{\partial^2 w}{\partial {x_1}^2} e^{-i\omega t} + \frac{\partial^2 w}{\partial {x_2}^2} e^{-i\omega t} + \frac{\omega^2}{c^2} w e^{-i\omega t} = 0,$$

which gives for w a Helmholtz equation

$$\Delta w + k^2 w = 0, \tag{2.4}$$

where the wave number $k = \omega/c$ is assumed to be real and positive. To summarize, the space dependent part $w : \Omega \subset \mathbb{R}^2 \to \mathbb{C}$ of any time-harmonic wave has to satisfy the Helmholtz equation (2.4) at every point of its open domain Ω.

In the case of scattering problems, the total wave field W can be viewed as the sum of the incident field W^i and the scattered field W^s as illustrated in Figure REF. Since the angular frequency ω of the scattered wave will be equal to that of the incident field, we can write

$$W^i = \mathrm{Re}\left\{w^i(x_1, x_2)e^{-i\omega t}\right\} \quad \text{and} \quad W^s = \mathrm{Re}\left\{w^s(x_1, x_2)e^{-i\omega t}\right\},$$

which yields

$$W = W^i + W^s = \mathrm{Re}\left\{\left(w^i(x_1, x_2) + w^s(x_1, x_2)\right)e^{-i\omega t}\right\}.$$

Hence the space dependent part $w^i(x_1, x_2) + w^s(x_1, x_2)$ has to satisfy the Helmholtz equation,

$$\Delta(w^i + w^s) + k^2(w^i + w^s) = 0.$$

The linearity of the Laplace operator Δ allows us to write this as

$$\left(\Delta w^i + k^2 w^i\right) + \left(\Delta w^s + k^2 w^s\right) = 0.$$

Since W^i is a wave, its space dependent part w^i satisfies the Helmholtz equation, and thus

$$\Delta w^s + k^2 w^s = 0.$$

In other words, w^s also is a solution to the Helmholtz equation.

In obstacle scattering we need to impose conditions for the solution of the Helmholtz equation on the boundary of the obstacle. Therefore, assume that the obstacle $D \subset \mathbb{R}^2$ is a bounded open subset such that $\mathbb{R}^2 \setminus \overline{D}$ is connected and that the boundary ∂D is sufficiently smooth. Let ν be a unit normal vector to ∂D directing to the exterior of D, and $d \in S^1$ the direction of propagation of the incident wave, see Figure 2.1 for an illustration. In the case of so-called sound-hard obstacles the boundary condition is of the form

$$\frac{\partial W}{\partial \nu} = \frac{\partial (W^i + W^s)}{\partial \nu} = 0 \quad \text{on } \partial D. \tag{2.5}$$

This type of boundary condition is called Neumann boundary condition, and physically it requires that the normal velocity of the wave vanishes on the boundary ∂D.

We notice that the condition (2.5) holds at every instant only if the space dependent part of W is zero on ∂D. Therefore we can write the condition as follows:

$$\frac{\partial w^s}{\partial \nu} = -\frac{\partial w^i}{\partial \nu} \quad \text{on } \partial D.$$

In other words, the scattered field can be considered as a wave field whose normal derivative cancels the normal derivative of the incident field on ∂D.

Finally, we require that the scattered field satisfies the Sommerfeld radiation condition

$$\lim_{r\to\infty} \sqrt{r} \left(\frac{\partial w^s}{\partial \nu} - ikw^s \right) = 0, \quad r = |x|,$$

where the limit is assumed to hold uniformly in all directions $x/|x|$. This condition was introduced by Sommerfeld [14] in 1912, and it ensures the uniqueness of the scattered field w^s and thus also the uniqueness of the total field. Physically it is related to the fact that the scattered radiation (wave motion) is emitted from the source to infinity, not from infinity to the source.

To summarize, our model for the acoustic obstacle scattering of time-harmonic incident plane waves ($w^i = e^{ikx\cdot d}$) is the exterior Neumann problem

$$\begin{aligned} \Delta w^s + k^2 w^s &= 0 \quad \text{in } \mathbb{R}^2 \setminus \overline{D}, \\ \frac{\partial w^s}{\partial \nu} &= g \quad \text{on } \partial D, \\ \lim_{r\to\infty} \sqrt{r} \left(\frac{\partial w^s}{\partial r} - ikw^s \right) &= 0, \quad r = |x|, \end{aligned} \tag{2.6}$$

where the function g is defined by $g(x) = -(\partial/\partial\nu)e^{ikd\cdot x}$. Essentially all of what follows is motivated by or directly related to this boundary value problem. In the analysis we will make some assumptions related for example to the smoothness of

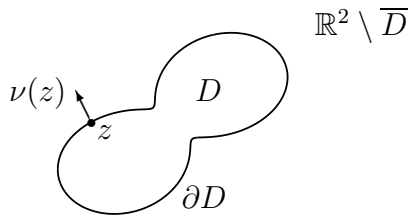

Figure 2.1: Open bounded subset $D \subset \mathbb{R}^2$ and its boundary ∂D. The vector $\nu(z)$ denotes the outward unit normal to ∂D at $z \in \partial D$.

∂D. These assumptions will be formulated in the forthcoming sections and separately for each result.

2.2 Preliminaries

Advanced mathematical analysis typically assumes some preliminary knowledge and results. This work is no exception. The aim of this section is to present the most important preliminary results and definitions that will be needed in the analysis of the boundary value problem (2.6). Most of the results are well known and hence we will not prove them but refer to existing literature.

2.2.1 Jordan arcs and curves in plane

To motivate the discussion of this subsection, consider an open bounded subset $D \subset \mathbb{R}^2$ and its boundary ∂D as illustrated in Figure 2.1. In terms of direct obstacle scattering D can be interpreted to model the impenetrable obstacle, the goal being to solve the scattered field in $\mathbb{R}^2 \setminus \overline{D}$. The approach of this thesis reduces the solving process to the computation of a line integral over the boundary curve ∂D. In order to compute this line integral we need a parametrization for the boundary curve. First we define the parametrization for general arc in $\mathbb{R}^2$ and the concept of a simple closed curve, a Jordan curve, which is of special interest in scattering theory; notice that the boundary ∂D is a Jordan curve.

Definition 2.2.1. *The image $\Gamma \subset \mathbb{R}^2$ of a continuous one-to-one mapping $x : [a,b] \subset \mathbb{R} \to \Gamma$ or $x : (a,b) \subset \mathbb{R} \to \Gamma$ is an* arc*, and the mapping x is a* parametrization *of this arc. In particular, $\Gamma \subset \mathbb{R}^2$ is a Jordan curve if there exists a parametrization x such that the mapping $t \mapsto x(t)$ is one-to-one on $[a,b)$ and $x(a) = x(b)$.*

It is often convenient to set smoothness conditions for a curve, for example, in order to apply Green's integral identities. Therefore, we define a concept of C^k-smooth arcs and curves.

Definition 2.2.2. *An arc is said to be C^k-smooth if it has a (C^k) parametrization $x(\cdot) = (x_1(\cdot), x_2(\cdot))$, where $x_1, x_2 \in C^k\big((a,b)\big)$ and $|x'(t)| > 0$ for all $t \in (a,b)$. In*

the case of a C^k-smooth Jordan curve we additionally require that $x^{(n)}(a) = x^{(n)}(b)$ for all $n \in \{0, 1, \dots k\}$.

Consider then a line integral over an arc or a Jordan curve Γ. Assume that Γ is C^1-smooth with a C^1 parametrization $x : [a, b] \to \Gamma$. Then the line integral of an integrable function $f : \Gamma \to \mathbb{R}$ over Γ is

$$\int_\Gamma f(x)ds(x) := \int_a^b f(x(t))|x'(t)|dt. \tag{2.7}$$

This is well-defined, since the value of the integral is independent of the choice of the C^1 parametrization x (proof is based on the chain rule and change of variables and can be found in most calculus textbooks, for example [6]). The definiton (2.7) can also be applied to the case of piecewise C^1-smooth boundary by first integrating over the smooth parts of the boundary and then summing these.

Denoting $x(t) = (x_1(t), x_2(t))$ the unit tangent vector at $x(t)$ is

$$\tau(x(t)) := \frac{1}{|x'(t)|}(x_1'(t), x_2'(t)) \tag{2.8}$$

provided that x is C^1. We notice that by choosing the parametrization appropriately the outward unit normal at $x(t)$ is given by

$$\nu(x(t)) = \frac{1}{|x'(t)|}(x_2'(t), -x_1'(t)), \tag{2.9}$$

since $\big(x_1'(t), x_2'(t)\big) \cdot \big(x_2'(t), -x_1'(t)\big) = 0$. Throughout this report ν will denote the outward unit normal to the Jordan curve in question.

Finally, we define the length of a C^1-smooth arc Γ with a C^1 parametrization $x : [a, b] \subset \mathbb{R} \to \Gamma$ as

$$l(\Gamma) := \int_a^b |x'(t)|dt, \tag{2.10}$$

which again is independent of the choice of x.

When establishing the existence of a solution of (2.6) we will analyze the behavior of certain line integrals at the vicinity of the boundary ∂D. More specifically, given $z \in \partial D$ we will have to estimate the line integral over the subarc of ∂D in the neighborhood of z. Therefore an appropriate parametrization for this subarc is necessary. The following lemma guarantees the existence of this kind of parametrization.

Lemma 2.2.3. *Assume that ∂D is a C^1-smooth Jordan curve and $z \in \partial D$. Then there exists $R > 0$ and a parametrization $y : (-\delta, \delta) \to \Gamma(z, \delta)$ given by*

$$y(\alpha) = z + \alpha\tau(z) + g_z(\alpha)\nu(z),$$

where $\Gamma(z,\delta) = \{x \in \partial D : x = y(\alpha) \text{ with some } \alpha \in (-\delta,\delta)\}$, $0 < \delta < R$, *and* $g_z \in C^1\big((-\delta,\delta)\big)$.

Proof. Let $z \in \partial D$. Without loss of generality we choose for ∂D a C^1 parametrization $x : [a,b] \to \partial D$ satisfying $z = x(0)$. Then for any $y \in \partial D$ we can write

$$y - z = \alpha\tau(z) + \beta\nu(z),$$

where

$$\begin{aligned}\alpha &= (y-z)\cdot\tau(z) = (x(s)-x(0))\cdot\tau(z) = \alpha(s), \quad \text{and}\\ \beta &= (y-z)\cdot\nu(z) = (x(s)-x(0))\cdot\nu(z) = \beta(s).\end{aligned}$$

In order to see that β can be represented as a function of $\alpha = \alpha(s)$ on some open interval, we show that the function α has an inverse α^{-1} on this interval, which then implies that β can be written as $\beta(\alpha^{-1}(\alpha(s))) = \beta \circ \alpha^{-1}(\alpha(s)) =: g_z(\alpha)$. Since

$$\frac{d\alpha}{ds}(s) = x'(s)\cdot\tau(z) = x'(s)\cdot\frac{x'(0)}{|x'(0)|},$$

and x' is continuous, there exists $r > 0$ such that $x'(s)\cdot x'(0) > 0$ for $s \in (-r,r)$. Hence $\frac{d\alpha}{ds}(s) > 0$ on $(-r,r)$ and the inverse function theorem implies that α has a C^1 inverse α^{-1} on $(-r,r)$. We have now established that there exists a subarc of ∂D that contains z as its interior point and has a parametrization of the form

$$y(\alpha(s)) = z + \alpha(s)\tau(z) + g_z(\alpha(s))\nu(z), \quad s \in (-r,r),$$

where g_z is a C^1 function since β and α^{-1} are C^1 functions. Since α is an increasing function on $(-r,r)$, we can omit the argument and write

$$y(\alpha) = z + \alpha\tau(z) + g_z(\alpha)\nu(z), \quad \alpha \in (\alpha(-r),\alpha(r)).$$

The result follows by choosing $R = \min\big\{|\alpha(-r)|, |\alpha(r)|\big\}$. □

2.2.2 Green's integral identity and unique continuation

Green's integral identities form a set of three equations that can be derived from the divergence theorem. They provide a valuable tool when analyzing, for example, solutions of Laplace and Helmholtz equations. We will need the first one of these identities in order to show that the exterior Neumann problem (2.6) has at most one solution.

Green's first identity in two dimensions is frequently formulated as follows.

Theorem 2.2.4. (Green's first identity) *Assume that $\Omega \subset \mathbb{R}^2$ is a bounded open set with C^1-smooth boundary $\partial\Omega$, $u \in C^1(\overline{\Omega})$, and $v \in C^2(\overline{\Omega})$. Then*

$$\int_\Omega v\Delta w dx = -\int_\Omega \operatorname{grad} v \cdot \operatorname{grad} w \, dx + \int_{\partial\Omega} v\frac{\partial w}{\partial \nu} ds. \tag{2.11}$$

The set $C^k(\overline{\Omega})$ denotes a set of functions that belong to $C^k(\Omega)$ and whose derivatives up to order k can be continuously extended from Ω to $\overline{\Omega}$.

The above formulation of Green's first identity is not very useful in terms of our analysis. More precisely, we would like to apply the identity to functions u and w that both belong to[1] $C^2(\Omega) \cap C(\overline{\Omega})$ and have normal derivatives on $\partial\Omega$ in the sense that the one-sided limits

$$\begin{aligned} \lim_{h\to 0+} \frac{\partial u}{\partial \nu(x)}(x - h\nu(x)) &= \lim_{h\to 0+} \nu(x) \cdot \operatorname{grad}\big(u(x - h\nu(x)\big), \text{ and similarly} \\ \lim_{h\to 0+} \frac{\partial v}{\partial \nu(x)}(x - h\nu(x)) &= \lim_{h\to 0+} \nu(x) \cdot \operatorname{grad}\big(v(x - h\nu(x)\big) \end{aligned} \tag{2.12}$$

exist uniformly. It can be shown, indeed, that Green's first identity (2.11) is applicable to these functions also. However, this requires that $\partial\Omega$ is assumed to be C^2-smooth.

The following theorem will be needed in establishing the uniqueness of the solution of (2.6). Notice that a function satisfying the Helmholtz equation meets the conditions of the theorem.

Theorem 2.2.5. (Unique Continuation Principle) *Let $\Omega \subset \mathbb{R}^n$ be an open connected set and $u : \Omega \to \mathbb{R}$ a twice continuously differentiable function satisfying*

$$|\Delta u(x)| \le C\big(|u(x)| + |\operatorname{grad} u(x)|\big), \quad x \in \Omega$$

with some constant $C > 0$. Then, if u vanishes in some open ball contained in Ω, it vanishes in the whole Ω.

Proof. For a proof, see e.g. [5, Lemma 8.5]. □

[1] The set $C^2(\Omega) \cap C(\overline{\Omega})$ denotes the set of functions that belong to $C^2(\Omega)$ and can be continuously extended from Ω to $\overline{\Omega}$.

2.3 Uniqueness of the scattering solution

We begin our analysis of the boundary value problem

$$\begin{aligned} \Delta w + k^2 w &= 0 \quad \text{in } \mathbb{R}^2 \setminus \overline{D}, \\ \frac{\partial w}{\partial \nu} &= g \quad \text{on } \partial D, \\ \lim_{r\to\infty} \sqrt{r}\left(\frac{\partial w}{\partial r} - ikw\right) &= 0, \quad r = |x|, \end{aligned} \tag{2.13}$$

by establishing the uniqueness of its solution, or, to be precise, we actually show that the problem has at most one solution. To do this we have to specify in which set we search for the solutions.

Since the solution w of (2.13) has to satisfy the Helmholtz equation, we require it to be twice continuously differentiable in $\mathbb{R}^2 \setminus \overline{D}$, that is, $w \in C^2(\mathbb{R}^2 \setminus \overline{D})$. Furthermore, because of the boundary condition we require that w possesses a normal derivative on ∂D in the sense that the limit

$$\lim_{h\to 0+} \frac{\partial w}{\partial \nu(x)}(x + h\nu(x)) = \lim_{h\to 0+} \nu(x) \cdot \operatorname{grad}(w(x + h\nu(x)), \quad x \in \partial D \tag{2.14}$$

exists uniformly. Finally, since we wish to apply Green's integral identity, we assume that ∂D is C^2-smooth and $w \in C(\mathbb{R}^2 \setminus D)$, i.e., w can be continuously extended from $\mathbb{R}^2 \setminus \overline{D}$ to $\mathbb{R}^2 \setminus D$ (see discussion in section 2.2.2). With these assumptions the solution w of (2.13) is unique as we shall show in this section.

The uniqueness of the solution is a reasonable property from the physical point of view and, on the other hand, it allows us to search for the solution by using any strategy or method; if we find a solution w of (2.13) that belongs to $C^2(\mathbb{R}^2 \setminus \overline{D}) \cap C(\mathbb{R}^2 \setminus D)$ and has a normal derivative on ∂D in the sense of uniformly existing limit (2.14), then we know that it is the unique solution of the problem.

Remark: The limit of the Sommerfeld radiation condition

$$\lim_{r\to\infty} \sqrt{r}\left(\frac{\partial w}{\partial r} - ikw\right) = 0 \tag{2.15}$$

is assumed to hold uniformly for all directions $x/|x|$.

The essential ingredients of the uniqueness proof are Rellich's lemma, Green's first identity (2.11), and the unique continuation principle (Theorem 2.2.5). We start with proving Rellich's lemma.

Lemma 2.3.1. (Rellich) *Denote* $\Omega_r = \{y \in \mathbb{R}^2 : |y| = r\}$. *If* $w \in C^2(\mathbb{R}^2 \setminus \overline{D})$ *is a*

solution to the Helmholtz equation, and

$$\lim_{r\to\infty}\int_{\Omega_r}|w(x)|^2ds(x)=0,\quad r=|x|, \tag{2.16}$$

then $w=0$ *in* $\mathbb{R}^2\setminus\overline{D}$.

Proof. The first thing to notice is that w can be expressed as a Fourier series expansion on Ω_r with sufficiently large r. Indeed, consider w in polar coordinates (r,θ) and notice that according to (2.16) there exists a constant $R>0$ such that $w(r,\cdot)\in L^2([0,2\pi])$ for $r>R$. Hence, for any $r>R$

$$w(r,\theta)=\sum_{n=-\infty}^{\infty}c_n(r)e^{in\theta}, \tag{2.17}$$

where

$$c_n(r)=\frac{1}{2\pi}\int_0^{2\pi}w(r,\phi)e^{-in\phi}d\phi.$$

Using the convenient way of parametrizing Ω_r with the complex-valued function $x=x(\phi)=re^{i\phi}$ we obtain

$$\begin{aligned}\int_{\Omega_r}|w(x)|^2ds(x)&=\int_0^{2\pi}|w(x(\phi))|^2|x'(\phi)|d\phi\\&=r\int_0^{2\pi}|w(x(\phi))|^2d\phi.\end{aligned} \tag{2.18}$$

According to Parseval's theorem

$$\int_0^{2\pi}|w(x(\phi))|^2d\phi=2\pi\sum_{n=-\infty}^{\infty}|c_n(r)|^2. \tag{2.19}$$

Combining (2.18) and (2.19) we have

$$\int_{\Omega_r}|w(x)|^2ds(x)=2\pi r\sum_{n=-\infty}^{\infty}|c_n(r)|^2.$$

Our assumption (2.16) now implies that

$$\lim_{r\to\infty}r|c_n(r)|^2=0 \tag{2.20}$$

for all $n\in\mathbb{Z}$.

The second step of the proof is to show that the coefficients $c_n(r)$ must be zero for each n. This will follow from (2.20) and the fact that w is a solution of the Helmholtz equation.

Recall that the Laplace operator Δ in polar coordinates is given by

$$\Delta(w(r,\phi)) = \left(\frac{\partial^2}{\partial r^2} + \frac{1}{r}\frac{\partial}{\partial r} + \frac{1}{r^2}\frac{\partial^2}{\partial \phi^2}\right) w(r,\phi).$$

Differentiating the Fourier series (2.17) term-by-term we obtain

$$\sum_{n=-\infty}^{\infty} \left(\frac{\partial^2}{\partial r^2} + \frac{1}{r}\frac{\partial}{\partial r} + \frac{1}{r^2}\frac{\partial^2}{\partial \phi^2} + k^2\right) \left(c_n(r)e^{in\theta}\right) = 0,$$

which yields

$$\sum_{n=-\infty}^{\infty} \left(c_n''(r) + \frac{1}{r}c_n'(r) + \left(k^2 - \frac{n^2}{r^2}\right) c_n(r)\right) e^{in\theta} = 0.$$

The functions $e^{in\theta}$ $(n = 0, \pm 1, \pm 2, \dots)$ form an orthonormal basis of $L^2([0, 2\pi])$, and thus each coefficient has to be individually zero, that is,

$$c_n''(r) + \frac{1}{r}c_n'(r) + \left(k^2 - \frac{n^2}{r^2}\right) c_n(r) = 0$$

for all $n \in \mathbb{Z}$. This is almost a Bessel equation, and setting $a_n(s) = c_n(s/k)$ we in fact obtain a Bessel equation

$$a_n''(s) + \frac{1}{s}a_n'(s) + \left(1 - \frac{n^2}{s^2}\right) a_n(s) = 0,$$

whose solutions are of the form

$$a_n(s) = \alpha_n J_n(s) + \beta_n Y_n(s),$$

where α_n and β_n are constants, and J_n and Y_n are Bessel and Neumann functions of order n, respectively. Functions J_n and Y_n have asymptotic expansions [1]

$$J_n(s) = \sqrt{\frac{2}{\pi s}} \cos\left(s - \frac{n\pi}{2} - \frac{\pi}{4}\right) + O\left(\frac{1}{s}\right), \quad \text{and}$$
$$Y_n(s) = \sqrt{\frac{2}{\pi s}} \cos\left(s - \frac{n\pi}{2} - \frac{\pi}{4}\right) + O\left(\frac{1}{s}\right),$$

as $s \to \infty$. From these expansions and equation (2.20) we conclude that

$$\lim_{r\to\infty} \left| \sqrt{\frac{2}{\pi k}} \left(\alpha_n \cos\left(kr - \frac{n\pi}{2} - \frac{\pi}{4}\right) + \beta_n \sin\left(kr - \frac{n\pi}{2} - \frac{\pi}{4}\right)\right) \right|^2 = 0.$$

This implies that $\alpha_n = \beta_n = 0$, i.e., $a_n = c_n = 0$ for each $n \in \mathbb{Z}$. Hence, $w = 0$ outside Ω_R.

Finally, according to the unique continuation principle, Theorem 2.2.5, applied to the real and imaginary parts of w respectively, it now follows that $w = 0$ in $\mathbb{R}^2 \setminus \overline{D}$. □

We are now in a position to prove that the boundary value problem (2.13) has at most one solution. The proof is based on Rellich's lemma and Green's first identity. Notice that we have to assume that ∂D is C^2-smooth in order to apply Green's first identity.

Theorem 2.3.2. (Uniqueness) *Assume that the boundary ∂D of the obstacle D is C^2-smooth. Let $u, v \in C^2(\mathbb{R}^2 \setminus \overline{D}) \cap C(\mathbb{R}^2 \setminus D)$, having normal derivatives on ∂D in the sense of uniformly existing limits* (2.12)*, be solutions to the exterior Neumann problem* (2.13)*. Then $u = v$.*

Proof. The strategy of the proof is to show that function $u - v$ satisfies all the assumptions of Lemma 2.3.1, which then implies that $u - v = 0$, i.e., $u = v$. In order to verify condition (2.16) for $w = u - v$ we will need Green's first identity.

Define $w = u - v$. Then w belongs to $C^2(\mathbb{R}^2 \setminus \overline{D})$. In addition, it is a solution to the Helmholtz equation, since

$$\begin{aligned} \Delta w + k^2 w &= \Delta(u - v) + k^2(u - v) \\ &= \Delta u + k^2 u - (\Delta v + k^2 v) \\ &= 0 - 0 \\ &= 0, \end{aligned}$$

and it satisfies the Sommerfeld radiation condition:

$$\begin{aligned} &\lim_{r\to\infty} \sqrt{r}\left(\frac{\partial w}{\partial r} - ikw\right) \\ &= \lim_{r\to\infty} \sqrt{r}\left(\frac{\partial (u - v)}{\partial r} - ik(u - v)\right) \\ &= \lim_{r\to\infty} \sqrt{r}\left(\frac{\partial u}{\partial r} - iku\right) - \lim_{r\to\infty} \sqrt{r}\left(\frac{\partial v}{\partial r} - ikv\right) \\ &= 0 - 0 \\ &= 0. \end{aligned}$$

Moreover, for the normal derivative of w on ∂D we have

$$\left.\frac{\partial w}{\partial \nu}\right|_{\partial D} = \left.\frac{\partial u}{\partial \nu}\right|_{\partial D} - \left.\frac{\partial v}{\partial \nu}\right|_{\partial D} = g - g = 0. \tag{2.21}$$

Now for the harder part, that is, to show that w satisfies (2.16). Using the fact that $|a-b|^2 = |a|^2 + |b|^2 - 2\mathrm{Re}(b\bar{a})$ for all $a, b \in \mathbb{C}$ yields

$$\left|\frac{\partial w}{\partial \nu} - ikw\right|^2 = \left|\frac{\partial w}{\partial \nu}\right|^2 + k^2|w|^2 + 2k\mathrm{Im}\left(w\frac{\partial \bar{w}}{\partial \nu}\right). \tag{2.22}$$

Define a circle $\Omega_r = \{y \in \mathbb{R}^2 \ : \ |y| = r\}$ and let ν denote its unit normal directed outwards. Since w satisfies the Sommerfeld radiation condition

$$\lim_{r\to\infty} \sqrt{r}\left(\frac{\partial w}{\partial \nu} - ikw\right) = 0,$$

where the limit holds uniformly, we have for any $\epsilon > 0$ a number $R > 0$ (not depending on x) such that

$$\left|\sqrt{r}\left(\frac{\partial w}{\partial \nu}(x) - ikw(x)\right)\right| < \epsilon$$

whenever $r > R$. Hence, for $r > R$,

$$\begin{aligned} 0 \le \int_{\Omega_r} \left|\frac{\partial w}{\partial \nu} - ikw\right|^2 ds &\le 2\pi r \sup_{x\in\Omega_r} \left|\frac{\partial w}{\partial \nu}(x) - ikw(x)\right|^2 \\ &= 2\pi \sup_{x\in\Omega_r} \left|\sqrt{r}\frac{\partial w}{\partial \nu}(x) - ikw(x)\right|^2 \\ &\le 2\pi\epsilon^2. \end{aligned}$$

Since $\epsilon > 0$ was arbitrary, we have

$$\lim_{r\to\infty} \int_{\Omega_r} \left|\frac{\partial w}{\partial \nu} - ikw\right|^2 ds = 0,$$

which, by (2.22), is equivalent to

$$\lim_{r\to\infty} \int_{\Omega_r} \left[\left|\frac{\partial w}{\partial \nu}\right|^2 + k^2|w|^2 + 2k\mathrm{Im}\left(w\frac{\partial \bar{w}}{\partial \nu}\right)\right] ds = 0.$$

Using properties of integrals and limits this can be written as

$$\lim_{r\to\infty} \int_{\Omega_r} \left(\left|\frac{\partial w}{\partial \nu}\right|^2 + k^2|w|^2\right) ds = -2k \lim_{r\to\infty} \mathrm{Im}\left(\int_{\Omega_r} w\frac{\partial \bar{w}}{\partial \nu} ds\right). \tag{2.23}$$

Next, choose r so large that D is contained inside the circle Ω_r, that is $|z| < r$ for all $z \in D$, and apply Green's first identity (2.11) in the region $D_r = \{y \in \mathbb{R}^2 \setminus \overline{D} \ :$

$|y| < r\}$ to obtain

$$\int_{\Omega_r \cup \partial D} w \frac{\partial \bar{w}}{\partial \nu} ds = \int_{D_r} (w \Delta \bar{w} + \operatorname{grad} w \cdot \operatorname{grad} \bar{w}) dS,$$

which is equivalent to

$$\int_{\Omega_r} w \frac{\partial \bar{w}}{\partial \nu} ds = -\int_{\partial D} w \frac{\partial \bar{w}}{\partial \nu} ds + \int_{D_r} \left(-k^2 |w|^2 + |\operatorname{grad} w|^2 \right) dS$$

since $\Delta \bar{w} = -k^2 \bar{w}$. We notice that the last term in this equation is real and, moreover, equation (2.21) implies that $(\partial \bar{w}/\partial \nu) = 0$ on ∂D. Hence

$$\operatorname{Im} \left(\int_{\Omega_r} w \frac{\partial \bar{w}}{\partial \nu} ds \right) = 0.$$

Inserting this into (2.23) yields

$$\lim_{r \to \infty} \int_{\Omega_r} \left(\left| \frac{\partial w}{\partial \nu} \right|^2 + k^2 |w|^2 \right) ds = 0.$$

From this we conclude that

$$\lim_{r \to \infty} \int_{\Omega_r} |w|^2 ds = 0.$$

We have now established that w satisfies all the assumptions of Lemma 2.3.1 and hence $w = 0$, i.e., $u = v$. □

2.4 Existence of the scattering solution

Having established in the previous section that the exterior Neumann problem

$$\begin{aligned} \Delta w + k^2 w &= 0 \quad \text{in } \mathbb{R}^2 \setminus \overline{D}, \\ \frac{\partial w}{\partial \nu} &= g \quad \text{on } \partial D, \\ \lim_{r \to \infty} \sqrt{r} \left(\frac{\partial w}{\partial r} - ikw \right) &= 0, \quad r = |x|, \end{aligned} \tag{2.24}$$

has at most one solution, it remains to show that there exists some function $w \in C^2(\mathbb{R}^2 \setminus \overline{D}) \cap C(\mathbb{R}^2 \setminus D)$ that has a normal derivative on ∂D in the sense of uniformly existing limit

$$\lim_{h \to 0+} \frac{\partial w}{\partial \nu(x)} (x + h\nu(x)) = \lim_{h \to 0+} \nu(x) \cdot \operatorname{grad} (w(x + h\nu(x)), \quad x \in \partial D$$

and satisfies (2.24). We will do this by using a method that belongs to the class of boundary integral equation methods. Using this method reduces our problem to finding a function $f \in C(\partial D)$ such that the so-called single-layer potential w defined by

$$w(x) = \int_{\partial D} \Phi(x-y) f(y) ds(y)$$

satisfies the boundary condition $\partial w/\partial \nu = g$ on ∂D. Here Φ is the *fundamental solution* of the Helmholtz equation.

We begin this section by proving the essential properties of the single-layer potential regarding its continuity and differentiability as well as its behavior on the boundary ∂D. Then in the second subsection we show that it solves the exterior Neumann problem (2.24).

2.4.1 The single-layer potential

In this subsection we will study regularity properties of the single-layer potential. The treatment is quite technical but the motivation becomes apparent in the following subsection, where we show that the single-layer potential solves the exterior Neumann problem (2.24).

Definition

The single-layer potential of interest in this work is based on the fundamental solution of the Helmholtz equation given by

$$\Phi(x) = \frac{i}{4} H_0^{(1)}(k|x|), \quad x \in \mathbb{R}^2 \setminus \{0\}, \tag{2.25}$$

where $H_0^{(1)}$ is the Hankel function of the first kind and order zero. We now define the single-layer potential $w : \mathbb{R}^2 \setminus \partial D \to \mathbb{C}$ as

$$w(x) := \int_{\partial D} \Phi(x-y) f(y) ds(y), \quad x \in \mathbb{R}^2 \setminus \partial D, \tag{2.26}$$

where $f \in C(\partial D)$ is called *density*. The set $D \subset \mathbb{R}^2$ denotes an open bounded set. Some of the following results further assume the boundary ∂D to be either C^1- or C^2-smooth. These assumptions are stated separately for each result.

Our first aim is to show that the single-layer potential w belongs to $C^2(\mathbb{R}^2 \setminus \overline{D}) \cap C(\mathbb{R}^2 \setminus D)$. In order to do this, we have to define what it means that w is continuous at $x \in \partial D$, since the integral in (2.26) is not even defined on ∂D. However, the integral exists in the sense of improper integral because of the logarithmic singularity

of Φ at the vicinity of zero. Thus we can define

$$w(x) = \lim_{l(\Gamma)\to 0} \int_{\partial D \setminus \Gamma} \Phi(x-y) f(y) ds(y), \quad x \in \partial D, \tag{2.27}$$

where Γ is a subarc of ∂D containing x as its interior point, and $l(\Gamma)$ is the length of Γ. The second aim is to investigate how the one-sided directional derivative of the single-layer potential behaves on the boundary ∂D.

In the analysis we will need some results concerning the asymptotic behavior of the Hankel functions. Hence we state these results which can be found for example in [1] or with a more rigorous analysis in [11].

$$H_0^{(1)}(z) = \sqrt{\frac{2}{\pi z}} e^{i(z-\pi/4)} \left[1 + O\left(\frac{1}{z}\right)\right] \quad \text{as } z \to \infty, \tag{2.28}$$

$$H_0^{(1)'}(z) = \sqrt{\frac{2}{\pi z}} e^{i(z+\pi/4)} \left[1 + O\left(\frac{1}{z}\right)\right] \quad \text{as } z \to \infty, \tag{2.29}$$

$$H_0^{(1)}(z) = \frac{2i}{\pi} \log z + O(1) \quad \text{as } z \to 0, \tag{2.30}$$

$$H_1^{(1)}(z) = \frac{2i}{\pi z} + O(1) \quad \text{as } z \to 0. \tag{2.31}$$

In addition to these asymptotic expansions, the equality

$$\frac{d}{dz} H_0^{(1)}(z) = -H_1^{(1)}(z) \tag{2.32}$$

will be used occasionally.

Regularity properties

We start with proving that the single-layer potential belongs to $C^2(\mathbb{R}^2 \setminus \overline{D}) \cap C(\mathbb{R}^2 \setminus D)$. In fact, it even belongs to $C^2(\mathbb{R}^2 \setminus \partial D) \cap C(\mathbb{R}^2)$ and proving this requires no extra effort so we formulate and prove the following result in this more general form.

Theorem 2.4.1. *Assume that ∂D is a C^1-smooth Jordan curve. The single-layer potential w is continuous in $\mathbb{R}^2$ and twice continuously differentiable in $\mathbb{R}^2 \setminus \partial D$.*

Proof. The continuity of w in $\mathbb{R}^2 \setminus \partial D$ follows from the continuity of Φ in $\mathbb{R}^2 \setminus \{0\}$, which is seen as follows. Let $x \in \mathbb{R}^2 \setminus \partial D$. Then for each $\epsilon > 0$ there exists $\delta > 0$

such that

$$\begin{aligned}
|w(x) - w(\hat{x})| &= \left| \int_{\partial D} \Phi(x-y) f(y) ds(y) - \int_{\partial D} \Phi(\hat{x}-y) f(y) ds(y) \right| \\
&= \left| \int_{\partial D} (\Phi(x-y) - \Phi(\hat{x}-y)) f(y) ds(y) \right| \\
&\leq \int_{\partial D} |\Phi(x-y) - \Phi(\hat{x}-y)||f(y)| ds(y) \\
&\leq \|f\|_\infty \int_{\partial D} |\Phi(x-y) - \Phi(\hat{x}-y)| ds(y) \\
&< \|f\|_\infty \int_{\partial D} \frac{\epsilon}{\|f\|_\infty l(\partial D)} ds(y) \\
&= \epsilon,
\end{aligned}$$

if $|x - \hat{x}| < \delta$. This implies the continuity of w in $\mathbb{R}^2 \setminus \partial D$.

Consider then the more difficult case $x \in \partial D$. To prove the continuity of w at x we define $\Gamma(x, \delta)$ as in Lemma 2.2.3 and

$$B_\delta(x) = \{z \in \mathbb{R}^2 \ : \ z = x + t\tau(x) + t\nu(x), \text{ where } |t| \leq \delta\} \tag{2.33}$$

and show that for any $\epsilon > 0$ there exists a $\delta > 0$ such that $|w(x) - w(\hat{x})| < \epsilon$ for all $\hat{x} \in B_\delta(x)$. We have for each $\hat{x} \in B_\delta(x)$

$$\begin{aligned}
|w(x) - w(\hat{x})| &= \left| \int_{\Gamma(x,\delta)} \Phi(x-y) f(y) ds(y) - \int_{\Gamma(x,\delta)} \Phi(\hat{x}-y) f(y) ds(y) \right. \\
&\qquad \left. + \int_{\partial D \setminus \Gamma(x,\delta)} (\Phi(x-y) - \Phi(\hat{x}-y)) f(y) ds(y) \right| \\
&\leq \int_{\Gamma(x,\delta)} |\Phi(x-y) f(y)| \, ds(y) + \int_{\Gamma(x,\delta)} |\Phi(\hat{x}-y) f(y)| \, ds(y) \\
&\qquad + \int_{\partial D \setminus \Gamma(x,\delta)} |(\Phi(x-y) - \Phi(\hat{x}-y)) f(y)| \, ds(y).
\end{aligned} \tag{2.34}$$

Our aim is to show that by choosing a sufficiently small $\delta > 0$ each of the integrals in the last expression becomes arbitrarily small. We consider first the second integral over $\Gamma(x, \delta)$. We write $\hat{x}$ and y as

$$\hat{x} = x + \hat{\alpha}\tau(x) + \hat{\beta}\nu(x) \quad \text{and} \quad y = x + \alpha\tau(x) + g_x(\alpha)\nu(x),$$

where $\tau(x)$ is the tangential unit vector of ∂D at x and the representation of y is

based on Lemma 2.2.3. Then, by using the Pythagorean theorem, we obtain

$$\begin{aligned}|\hat{x}-y|^2 &= |(\hat{\alpha}-\alpha)\tau(x)+(\hat{\beta}-g_x(\alpha))\nu(x)|^2\\ &= |\hat{\alpha}-\alpha|^2+|\hat{\beta}-g_x(\alpha)|^2\\ &\geq |\hat{\alpha}-\alpha|^2,\end{aligned}$$

that is, $|\hat{x}-y|\geq|\hat{\alpha}-\alpha|$. Choosing δ so small that $|\hat{x}-y|<1$ yields

$$|\log|\hat{x}-y||\leq|\log|\hat{\alpha}-\alpha||$$

for all $\hat{x},y\in B_\delta(x)$. From the asymptotic form (2.30) we conclude that for δ sufficiently small, there exists a constant $c_1>0$ such that

$$|\Phi(\hat{x}-y)|\leq c_1|\log|\hat{x}-y||\leq c_1|\log|\hat{\alpha}-\alpha||$$

for all $\hat{x}\in B_\delta(x)$. Thus

$$\begin{aligned}\int_{\Gamma(x,\delta)}|\Phi(\hat{x}-y)f(y)|ds(y) &\leq \|f\|_\infty\int_{\Gamma(x,\delta)}|\Phi(\hat{x}-y)|ds(y)\\ &\leq c_1\|f\|_\infty\int_{-\delta}^{\delta}|\log|\hat{\alpha}-\alpha||d\alpha.\end{aligned}$$

Since the logarithmic singularity is integrable in the sense of improper integral, taking δ sufficiently small yields

$$\int_{\Gamma(x,\delta)}|\Phi(\hat{x}-y)f(y)|ds(y)\leq c_1\|f\|_\infty\int_{-\delta}^{\delta}|\log|\hat{\alpha}-\alpha||d\alpha<\epsilon/3. \tag{2.35}$$

The first integral over $\Gamma(x,\delta)$ in (2.34) can be made arbitrarily small by choosing a sufficiently small $\delta>0$, since, as already pointed out, the integral in (2.26) exists in the sense of improper integral according to (2.27). This implies that

$$\int_{\Gamma(x,\delta)}|\Phi(x-y)f(y)|ds(y)<\epsilon/3 \tag{2.36}$$

for $\delta>0$ sufficiently small. Moreover, since Φ is continuous in $\partial D\setminus\Gamma(x,\delta)$ for any $\delta>0$, we have

$$\int_{\partial D\setminus\Gamma(x,\delta)}|(\Phi(x-y)-\Phi(\hat{x}-y))f(y)|\,ds(y)<\epsilon/3 \tag{2.37}$$

for δ sufficiently small. Hence, choosing δ such that inequalities (2.35)-(2.37) are

satisfied we see from (2.34) that

$$|w(x) - w(\hat{x})| < \epsilon \quad \text{if} \quad |x - \hat{x}| < \delta.$$

Thus w is continuous in $\mathbb{R}^2$.

To establish that w is twice continuously differentiable in $\mathbb{R}^2 \setminus \overline{D}$, we notice that Φ is twice (or even infinitely) continuously differentiable in $\mathbb{R}^2 \setminus \{0\}$ and therefore we can differentiate under the integral to get

$$\frac{\partial^2}{\partial x_j^2} w(x) = \int_{\partial D} \frac{\partial^2}{\partial x_j^2} \Phi(x-y) f(y) ds(y), \quad x \in \mathbb{R}^2 \setminus \overline{D},$$

for $j = 1, 2$. These integrals exist and define continuous functions of x, since Φ is infinitely differentiable in $\mathbb{R}^2 \setminus \{0\}$. □

In addition to the single-layer potential the so-called double-layer potential $v : \mathbb{R}^2 \to \mathbb{C}$, defined by

$$v(x) = \int_{\partial D} \frac{\partial \Phi(x-y)}{\partial \nu(y)} f(y) ds(y), \tag{2.38}$$

where $f \in C(\partial D)$, is of special interest in scattering theory. Despite this fact the double-layer potential is not very essential in terms of our purposes. However, the well-known result of discontinuity, or "jump relation", of the double-layer potential on ∂D, is useful in proving the result concerning the normal derivative of the single-layer potential on ∂D. Hence we state this jump relation.

Lemma 2.4.2. *Assume that ∂D is a C^2-smooth Jordan curve. Then*

$$\lim_{h \to 0+} v(x + h\nu(x)) = \int_{\partial D} \frac{\partial \Phi(x-y)}{\partial \nu(y)} f(y) ds(y) + \frac{1}{2} f(x), \quad x \in \partial D. \tag{2.39}$$

Proof. For a proof, see e.g. [13, Theorem 2.5.2]. □

It has been shown that the single-layer potential w with merely continuous density f has not necessarily a derivative on ∂D ([4] and references therein). However, as shown in the following theorem, w has a normal derivative on ∂D in the sense that the limit

$$\frac{\partial w_+}{\partial \nu}(x) := \lim_{h \to 0+} \frac{\partial w}{\partial \nu(x)}(x + h\nu(x)) = \lim_{h \to 0+} \nu(x) \cdot \operatorname{grad}(w(x + h\nu(x)), \quad x \in \partial D$$

exists uniformly. Notice that there is a same type of "jump" in the normal derivative of w as is in the double-layer potential on ∂D.

Theorem 2.4.3. *Assume that ∂D is a C^2-smooth Jordan curve and $f \in C(\partial D)$.*

Then the normal derivative $\frac{\partial w_+}{\partial \nu}$ *of the single-layer potential* w *exists on* ∂D *and*

$$\frac{\partial w_+}{\partial \nu}(x) = \int_{\partial D} \frac{\partial \Phi(x-y)}{\partial \nu(x)} f(y) ds(y) - \frac{1}{2} f(x), \quad x \in \partial D. \tag{2.40}$$

Proof. Let $x \in \partial D$ and define

$$g(\hat{x}) = \int_{\partial D} \left(\frac{\partial}{\partial \nu(y)} + \frac{\partial}{\partial \nu(x)} \right) \Phi(\hat{x}-y) f(y) ds(y), \quad \hat{x} \in \mathbb{R}^2.$$

The integral exists for $\hat{x} \in \partial D$ also, since the functions

$$\frac{\partial}{\partial \nu(y)} \Phi(\hat{x}-y) \quad \text{and} \quad \frac{\partial}{\partial \nu(x)} \Phi(\hat{x}-y)$$

are continuous for $\hat{x}, y \in \partial D$, see [13, Section 2.5] for details. Now we have

$$\frac{\partial w_+}{\partial \nu(x)}(\hat{x}) = -v(\hat{x}) + g(\hat{x}), \quad \hat{x} \in \mathbb{R}^2 \setminus \overline{D},$$

where v is the double-layer potential given by (2.38). The strategy of the proof is to show that g is continuous at x along the normal line $x + h\nu(x)$, $h > 0$, and then apply the jump relation of v, Lemma 2.4.2.

To establish the continuity of g at x along the normal line we write $\hat{x} = x + h\nu(x)$ and show that for each $\epsilon > 0$ there exists $\delta > 0$ such that

$$|g(\hat{x}) - g(x)| < \epsilon, \quad \text{if } 0 < h < \delta.$$

Using the notations of Lemma 2.2.3 we have that

$$\begin{aligned} |g(\hat{x}) - g(x)| \leq & \left| \int_{\partial D \setminus \Gamma(x,\delta)} \left[\left(\frac{\partial}{\partial \nu(y)} + \frac{\partial}{\partial \nu(x)} \right) \Phi(\hat{x}-y) \right. \right. \\ & \left. \left. - \left(\frac{\partial}{\partial \nu(y)} + \frac{\partial}{\partial \nu(x)} \right) \Phi(x-y) \right] f(y) ds(y) \right| \\ & + \left| \int_{\Gamma(x,\delta)} \left(\frac{\partial}{\partial \nu(y)} + \frac{\partial}{\partial \nu(x)} \right) \Phi(\hat{x}-y) f(y) ds(y) \right| \\ & + \left| \int_{\Gamma(x,\delta)} \left(\frac{\partial}{\partial \nu(y)} + \frac{\partial}{\partial \nu(x)} \right) \Phi(x-y) f(y) ds(y) \right| \end{aligned} \tag{2.41}$$

The first term on the right side will be less than $\epsilon/3$ if $\delta > 0$ is taken small enough, since

$$\left(\frac{\partial}{\partial \nu(y)} + \frac{\partial}{\partial \nu(x)} \right) \Phi(\hat{x}-y) = \frac{ik}{4} H_1^{(1)}(k|\hat{x}-y|) \frac{(\nu(y)-\nu(x)) \cdot (\hat{x}-y)}{|\hat{x}-y|}$$

defines a continuous function on $B_\delta(x) \times \partial D \setminus \Gamma(x,\delta)$, where $B_\delta(x)$ is defined analogously to (2.33). To estimate the second term we notice from (2.31) that $tH_1^{(1)}(t) = \frac{2i}{\pi} + O(t)$ as $t \to 0$, which means that there exist $c > 0$ and $\delta > 0$ such that

$$\left| \left(\frac{\partial}{\partial \nu(y)} + \frac{\partial}{\partial \nu(x)} \right) \Phi(\hat{x} - y) \right| \leq c \frac{|(\nu(y) - \nu(x)) \cdot (\hat{x} - y)|}{|\hat{x} - y|^2}$$

if $|\hat{x} - y| < \delta$. Hence, writing y as $y(\alpha) = x + \alpha\tau(x) + g_x(\alpha)\nu(x)$ according to Lemma 2.2.3 we have

$$|\hat{x} - y| = |(h - g_x(\alpha))\nu(x) - \alpha\tau(x)| = \sqrt{(h - g_x(\alpha))^2 + \alpha^2} \geq |\alpha|,$$

and $|\nu(y) - \nu(x)| < c'|\alpha|$ for all $|\alpha| < \delta$ with some $c', \delta > 0$. Hence

$$\begin{aligned}
&\left| \int_{\Gamma(x,\delta)} \left(\frac{\partial}{\partial \nu(y)} + \frac{\partial}{\partial \nu(x)} \right) \Phi(\hat{x} - y) f(y) ds(y) \right| \\
&\leq cc' \|f\|_{\infty,\partial D} \int_{\Gamma(x,\delta)} \frac{|\nu(y) - \nu(x)|}{|\hat{x} - y|} ds(y) \\
&\leq cc' \|f\|_{\infty,\partial D} \int_{-\delta}^{\delta} \frac{|\alpha|}{|\alpha|} d\alpha \\
&\leq 2\delta cc' \|f\|_{\infty,\partial D} \\
&< \epsilon/3,
\end{aligned}$$

if δ is sufficiently small. Finally, the last term in (2.41) is also less than $\epsilon/3$ if δ is sufficiently small since, provided that ∂D is C^2-smooth,

$$\frac{\partial \Phi(x - y)}{\partial \nu(y)} \quad \text{and} \quad \frac{\partial \Phi(x - y)}{\partial \nu(x)}$$

are continuous functions of x and y on ∂D (for details, see [13, Section 2.5]). Thus we have established the continuity of g at x along the normal line. Now the theorem follows by applying the jump relation to the double-layer potential v, Lemma 2.4.2:

$$\begin{aligned}
\frac{\partial w_+}{\partial \nu}(x) &= \lim_{h \to 0+} \frac{\partial w}{\partial \nu(x)}(x + h\nu(x)) \\
&= \lim_{h \to 0+} \big(-v(x + h\nu(x)) + g(x + h\nu(x)) \big) \\
&= -\left(\int_{\partial D} \frac{\partial \Phi(x - y)}{\partial \nu(y)} + \frac{1}{2} f(x) \right) \\
&\quad + \int_{\partial D} \left(\frac{\partial}{\partial \nu(y)} + \frac{\partial}{\partial \nu(x)} \right) \Phi(x - y) f(y) ds(y) \\
&= \int_{\partial D} \frac{\partial \Phi(x - y)}{\partial \nu(x)} f(y) ds(y) - \frac{1}{2} f(x).
\end{aligned}$$

□

2.4.2 Solution as a single-layer potential representation

Next we shall show that the unique solution of the boundary value problem (2.24) can be determined by an integral over the boundary ∂D, that is, by the single-layer potential introduced in the previous subsection. This is a remarkable result especially from the numerical point of view since it both reduces the dimension of the problem and enables us to determine the function defined on an infinite domain as an integral over a compact set.

Although the fundamental solution Φ solves the Helmholtz equation and satisfies Sommerfeld radiation condition, it is not (necessarily) a solution to the exterior Neumann problem (2.24). However, the single-layer potential of the form

$$w(x) = \int_{\partial D} \Phi(x-y) f(y) ds(y), \quad x \in \mathbb{R}^2 \setminus \overline{D}$$

can be modified to satisfy the exterior Neumann problem by choosing the density $f \in C(\partial D)$ appropriately.

It is rather straightforward to show that the single-layer potential with any continuous density $f \in C(\partial D)$ satisfies the Helmholtz equation and the Sommerfeld radiation condition.

Theorem 2.4.4. *The single-layer potential w solves the Helmholtz equation in $\mathbb{R}^2 \setminus \overline{D}$.*

Proof. Since Φ is two times continuously differentiable in $\mathbb{R}^2 \setminus \{0\}$, we can differentiate under the integral sign to get

$$\begin{aligned} \Delta w(x) + k^2 w(x) &= \int_{\partial D} \Delta\Phi(x-y) f(y) ds(y) + \int_{\partial D} k^2 \Phi(x-y) f(y) ds(y) \\ &= \int_{\partial D} \underbrace{(\Delta\Phi(x-y) + k^2\Phi(x-y))}_{=0, \text{ if } x \neq y} f(y) ds(y) \\ &= 0 \end{aligned}$$

for all $x \in \mathbb{R}^2 \setminus \overline{D}$. □

Theorem 2.4.5. *The single-layer potential w satisfies the Sommerfeld radiation condition.*

Proof. We show first that Φ satisfies the Sommerfeld radiation condition. Denoting

$r = |x|$ and using the asymptotic expansions (2.28) and (2.29) we have

$$\begin{aligned}
&\sqrt{r}\left(\frac{\partial \Phi}{\partial r}(x) - ik\Phi(x)\right) \\
&= \sqrt{r}\left(\frac{k}{4}\sqrt{\frac{2}{\pi kr}}ie^{i(kr+\pi/4)}\left[1 + O\left(\frac{1}{r}\right)\right]\right. \\
&\qquad \left. + \frac{k}{4}\sqrt{\frac{2}{\pi kr}}e^{i(kr-\pi/4)}\left[1 + O\left(\frac{1}{r}\right)\right]\right) \\
&= \frac{\sqrt{2k}}{4\pi}e^{i(kr-\pi/4)}O\left(\frac{1}{r}\right), \quad \text{as } r \to \infty,
\end{aligned}$$

where we have used the fact that $ie^{i(kr+\pi/4)} = -e^{i(kr-\pi/4)}$. From this we conclude that the limit

$$\lim_{r\to\infty} \sqrt{r}\left(\frac{\partial \Phi}{\partial r} - ik\Phi\right) = 0, \quad r = |x|, \tag{2.42}$$

exists uniformly in all directions $x/|x|$ and hence Φ satisfies the Sommerfeld radiation condition.

It follows that

$$\begin{aligned}
&\lim_{r\to\infty} \sqrt{r}\left(\frac{\partial w}{\partial r}(x) - ikw(x)\right) \\
&= \lim_{r\to\infty}\left(\int_{\partial D} \sqrt{r}\frac{\partial \Phi}{\partial r}(x-y)f(y)ds(y) - \int_{\partial D} ik\sqrt{r}\Phi(x-y)f(y)ds(y)\right) \\
&= \lim_{r\to\infty}\left(\int_{\partial D}\left[\sqrt{r}\left(\frac{\partial \Phi}{\partial r}(x-y) - ik\Phi(x-y)\right)\right]f(y)ds(y)\right) \\
&= 0
\end{aligned}$$

since $r = |x| \to \infty$ implies $|x - y| \to \infty$ and (2.42) holds uniformly and the continuous function $f \in C(\partial D)$ has a maximum in the compact set ∂D. □

In the preceding results we assumed the density f only to be continuous. This clearly is not sufficient if we want the single-layer potential w to satisfy the Neumann boundary condition. Theorem 2.4.3 gives us essential information in terms of how to set the boundary condition using the single-layer potential. With the aid of that result we can finally establish that the single-layer potential with appropriately chosen density f solves the exterior Neumann problem (2.24). It is worth emphasizing, however, that the following result gives no information regarding the existence and uniqueness of the density.

Theorem 2.4.6. *Assume that ∂D is C^2-smooth. The* single-layer potential w *de-*

fined by

$$w(x) = \int_{\partial D} \Phi(x-y) f(y) ds(y), \quad x \in \mathbb{R}^2 \setminus \overline{D} \tag{2.43}$$

is a solution to the exterior Neumann problem (2.24) *if* $f \in C(\partial D)$ *satisfies the integral equation*

$$\left(\frac{1}{2} I - A\right) f = -g, \tag{2.44}$$

where the operator $A : C(\partial D) \to C(\partial D)$ *is given by*

$$(Af)(x) = \int_{\partial D} \frac{\partial \Phi(x-y)}{\partial \nu(x)} f(y) ds(y), \quad x \in \partial D. \tag{2.45}$$

Proof. We already know from Theorems 2.4.4 and 2.4.5 that w is a solution to the Helmholtz equation and satisfies the Sommerfeld radiation condition. Using (2.40) the Neumann boundary condition can be written as

$$\int_{\partial D} \frac{\partial \Phi(x-y)}{\partial \nu(x)} f(y) ds(y) - \frac{1}{2} f(x) = g.$$

But this is equivalent to (2.44) and the theorem follows. □

As already mentioned, the above result gives no information about the existence of a density $f \in C(\partial D)$ satisfying (2.44). The existence can be established using the theory of compact operators including the Riesz-Fredholm theory. We will not go into details of this theory, but give a sketch of a proof.

Theorem 2.4.7. *Assume that* ∂D *is* C^2*-smooth. Then the integral equation* (2.44) *is solvable (not necessarily uniquely).*

Proof. To be consistent with the standard formulation of the Riesz-Fredholm theory, we consider the solvability of equation

$$(I - 2A) f = -2g, \tag{2.46}$$

which clearly is equivalent to (2.44).

The strategy of the proof is to show that the operator $2A$ is compact and then apply the Riesz-Fredholm theory to (2.46). The compactness of A, and hence the compactness of $2A$, follows from the fact that any operator $K : C[a,b] \to C[c,d]$ defined by

$$(Kh)(t) = \int_a^b k(t,s) h(s) ds, \quad t \in [c,d],$$

with kernel $k \in C([c,d] \times [a,b])$ is compact. This well-known result is immediately applicable to the operator A, since the integral over ∂D reduces to an integral over

a real interval $[a, b]$ and the kernel of A is given by

$$\phi(t,s) := \frac{\partial \Phi(x(t) - x(s))}{\partial \nu(x(t))}, \quad s, t \in [a, b],$$

which is continuous provided that ∂D is C^2-smooth.

Now the Riesz-Fredholm theory implies that (2.46) is solvable. The details can be found for example in [4], where the analysis is carried out in $\mathbb{R}^3$ but is almost directly applicable to $\mathbb{R}^2$ also. □

2.5 The far field pattern

We conclude this section with an important result regarding the scattered field. This result tells us how the amplitude of the scattered wave asymptotically depends on the observation direction and it is of special interest in the *inverse* scattering problem, where the aim is to reconstruct the obstacle (or the boundary value problem) from the knowledge of the so-called far field pattern, or scattering amplitude. We first state the well-known Green's representation formula and prove two lemmas needed in the proof of the main result.

Theorem 2.5.1. *Assume that ∂D is C^2-smooth, and $w \in C^2(\mathbb{R}^2 \setminus \overline{D}) \cap C(\mathbb{R}^2 \setminus D)$ satisfies the Sommerfeld radiation condition and the Helmholtz equation in $\mathbb{R}^2 \setminus \overline{D}$. Moreover assume that w has a normal derivative on ∂D in the sense that the limit*

$$\lim_{h \to 0+} \frac{\partial w}{\partial \nu(x)}(x + h\nu(x)) = \lim_{h \to 0+} \nu(x) \cdot \operatorname{grad}(w(x + h\nu(x))), \quad x \in \partial D$$

exists uniformly. Then Green's representation formula

$$w(x) = \int_{\partial D} \left(w(y) \frac{\partial \Phi(x-y)}{\partial \nu(y)} - \frac{\partial w}{\partial \nu}(y) \Phi(x-y) \right) ds(y), \quad x \in \mathbb{R}^2 \setminus \overline{D} \tag{2.47}$$

is valid.

Proof. We refer to [3, Theorem 2.4.1]. □

Lemma 2.5.2. *Assume that $x \in \mathbb{R}^2$ and $y \in \partial D$, where $D \subset \mathbb{R}^2$ is a bounded set. Then $|x - y|$ has an asymptotic form*

$$|x - y| = |x| - \hat{x} \cdot y - O\left(\frac{1}{|x|}\right) \quad \text{as } |x| \to \infty, \tag{2.48}$$

where $\hat{x} = x/|x|$.

Proof. According to Taylor's theorem the function $t \mapsto \sqrt{1+t}$ can be written as

the convergent series

$$\sqrt{1+t} = 1 + \frac{1}{2}t - \frac{1}{8}t^2 + \frac{1}{16}t^3 - \frac{5}{128}t^4 + \dots \tag{2.49}$$

for all $t \in (-1, 1)$. Writing

$$|x-y| = \sqrt{|x|^2 - 2x\cdot y + |y|^2} = |x|\sqrt{1 + \left(\frac{|y|^2}{|x|^2} - \frac{2}{|x|}\hat{x}\cdot y\right)}, \tag{2.50}$$

we can apply (2.49) to the square root expression provided that

$$\left|\frac{|y|^2}{|x|^2} - \frac{2}{|x|}\hat{x}\cdot y\right| < 1.$$

This is indeed satisfied by taking $|x|$ sufficiently large, since

$$\begin{aligned}\left|\frac{|y|^2}{|x|^2} - \frac{2}{|x|}\hat{x}\cdot y\right| &= \frac{1}{|x|}\left|\frac{|y|^2}{|x|} - 2\hat{x}\cdot y\right| \\ &\le \frac{1}{|x|}\left(\frac{|y|^2}{|x|} + 2|y|\right) \to 0 \quad \text{as } |x| \to \infty,\end{aligned}$$

where we have used the Cauchy-Schwarz inequality $|\hat{x}\cdot y| \le |\hat{x}||y| = |y|$ and the fact that $|y|$ is bounded for $y \in \partial D$. Thus we can write the square root in (2.50) with the aid of (2.49) as

$$\begin{aligned}&|x|\sqrt{1 + \left(\frac{|y|^2}{|x|^2} - \frac{2}{|x|}\hat{x}\cdot y\right)} \\ &= |x|\left[1 + \frac{1}{2}\left(\frac{|y|^2}{|x|^2} - \frac{2}{|x|}\hat{x}\cdot y\right) - \frac{1}{8}\left(\frac{|y|^2}{|x|^2} - \frac{2}{|x|}\hat{x}\cdot y\right)^2 + \cdots\right] \\ &= |x| - \hat{x}\cdot y + \frac{1}{2}\frac{|y|^2}{|x|} + O\left(\frac{1}{|x|}\right) \\ &= |x| - \hat{x}\cdot y + O\left(\frac{1}{|x|}\right), \quad \text{as } |x| \to \infty.\end{aligned}$$

□

Lemma 2.5.3. *Assume that $x \in \mathbb{R}^2$ and $y \in \partial D$, where $D \subset \mathbb{R}^2$ is a bounded set. Then we have the asymptotic form*

$$\frac{e^{ik|x-y|}}{\sqrt{|x-y|}} = \frac{e^{ik|x|}}{\sqrt{|x|}}\left(e^{-ik\hat{x}\cdot y} + O\left(\frac{1}{|x|}\right)\right) \tag{2.51}$$

as $|x| \to \infty$. Here $\hat{x} = x/|x|$.

Proof. The strategy of the proof is to show that there exists a constant $M > 0$ such that

$$\left| \frac{e^{ik|x-y|}}{\sqrt{|x-y|}} - \frac{e^{ik(|x|-\hat{x}\cdot y)}}{\sqrt{|x|}} \right| \leq \frac{M}{|x|^{3/2}}$$

whenever $|x|$ is sufficiently large. From the previous lemma we see that

$$\begin{aligned} \left| \frac{e^{ik|x-y|}}{\sqrt{|x-y|}} - \frac{e^{ik(|x|-\hat{x}\cdot y)}}{\sqrt{|x|}} \right| &= \left| \frac{e^{ik(|x|-\hat{x}\cdot y+O(1/|x|))}}{\sqrt{|x-y|}} - \frac{e^{ik(|x|-\hat{x}\cdot y)}}{\sqrt{|x|}} \right| \\ &= \left| e^{ik(|x|-\hat{x}\cdot y)} \right| \left| \frac{e^{O(1/|x|)}}{\sqrt{|x-y|}} - \frac{1}{\sqrt{|x|}} \right| \\ &= \left| \frac{\sqrt{|x|}e^{O(1/|x|)} - \sqrt{|x-y|}}{\sqrt{|x|}\sqrt{|x-y|}} \right| \end{aligned}$$

as $|x| \to \infty$. Again, from the previous lemma and the Taylor series (2.49) we have that

$$\begin{aligned} \sqrt{|x-y|} &= \sqrt{|x| - \hat{x}\cdot y + O(1/|x|)} \\ &= \sqrt{|x|}\sqrt{1 + \left(O\left(\frac{1}{|x|^2}\right) - \frac{\hat{x}\cdot y}{|x|} \right)} \\ &= \sqrt{|x|}\left(1 + \frac{1}{2}\left(O\left(\frac{1}{|x|^2}\right) - \frac{\hat{x}\cdot y}{|x|} \right) - \frac{1}{8}\left(O\left(\frac{1}{|x|^2}\right) - \frac{\hat{x}\cdot y}{|x|} \right)^2 + \cdots \right) \\ &= \sqrt{|x|}\left(1 + O\left(\frac{1}{|x|}\right) \right) \\ &= \sqrt{|x|} + O\left(\frac{1}{\sqrt{|x|}}\right) \end{aligned}$$

as $|x| \to \infty$. Moreover,

$$\begin{aligned} e^{O(1/|x|)} &= \sum_{n=0}^{\infty} \frac{O(1/|x|)^n}{n!} \\ &= 1 + O\left(\frac{1}{|x|}\right) + O\left(\frac{1}{|x|^2}\right) + \cdots \\ &= 1 + O\left(\frac{1}{|x|}\right) \end{aligned}$$

as $|x| \to \infty$. Thus

$$\begin{aligned}\left|\frac{\sqrt{|x|}e^{O(1/|x|)}-\sqrt{|x-y|}}{\sqrt{|x|}\sqrt{|x-y|}}\right| &= \frac{\left|\sqrt{|x|}+O(1/\sqrt{|x|})-\sqrt{|x|}+O(1/\sqrt{|x|})\right|}{\big||x|+O(1)\big|}\\ &= \frac{\left|O(1/\sqrt{|x|})\right|}{\big||x|+O(1)\big|}\\ &\le \frac{M_1/\sqrt{|x|}}{|x|-M_2}\\ &= \frac{M_1}{|x|^{3/2}-\sqrt{|x|}M_2}\\ &= \frac{1}{|x|^{3/2}}\,\frac{M_1}{1-M_2/|x|}\end{aligned}$$

for some constants $M_1, M_2 > 0$ and $|x|$ sufficiently large. The assertion now follows since $|x| \ge 2M_2$ implies

$$\frac{1}{|x|^{3/2}}\,\frac{M_1}{1-M_2/|x|} \le \frac{2M_1}{|x|^{3/2}}.$$

□

Now we are ready to introduce the concept of far field pattern. The proof is somewhat technical but the essential idea and interpretation of the far field pattern is illustrated in Figure 2.2.

Theorem 2.5.4. *Under the assumptions of Theorem 2.5.1 we have: given a direction $\varphi \in S^1$ of observation, the solution w of the exterior Neumann problem* (2.24) *has an asymptotic form*

$$w(r\varphi) = \frac{e^{ikr}}{\sqrt{r}}F_D(\varphi; d, k) + O\left(\frac{1}{r^{3/2}}\right), \quad r \to \infty, \tag{2.52}$$

where the coefficient F_D, called the far field pattern *of D, is given by*

$$\frac{e^{i\pi/4}}{\sqrt{8k\pi}}\int_{\partial D}\left(w(y)\frac{\partial e^{-ik\varphi\cdot y}}{\partial\nu(y)} - \frac{\partial w}{\partial\nu}(y)e^{-ik\varphi\cdot y}\right)ds(y). \tag{2.53}$$

Proof. Since $|x| \to \infty$ implies $|x-y| \to \infty$ for any $y \in \partial D$, we can use (2.28) and

the preceding lemma to obtain

$$\begin{aligned}\Phi(x-y) &= \frac{i}{4}H_0^{(1)}(k|x-y|)\\ &= \frac{i}{4}\sqrt{\frac{2}{k\pi}}\frac{e^{i(k|x-y|-\pi/4)}}{\sqrt{|x-y|}}\left(1+O\left(\frac{1}{|x|}\right)\right)\\ &= \frac{ie^{-i\pi/4}}{\sqrt{8k\pi}}\frac{e^{ik|x|}}{\sqrt{|x|}}\left(e^{-ik\hat{x}\cdot y}+O\left(\frac{1}{|x|}\right)\right)\left(1+O\left(\frac{1}{|x|}\right)\right)\\ &= \frac{e^{i\pi/4}}{\sqrt{8k\pi}}\frac{e^{ik|x|}}{\sqrt{|x|}}\left(e^{-ik\hat{x}\cdot y}+O\left(\frac{1}{|x|}\right)\right) \quad \text{as } |x|\to\infty, \end{aligned} \tag{2.54}$$

where we have used the fact that $ie^{-i\pi/4} = e^{i\pi/4}$. Furthermore, the preceding lemma implies that

$$\frac{\partial\Phi(x-y)}{\partial\nu(y)} = \frac{e^{i\pi/4}}{\sqrt{8k\pi}}\frac{e^{ik|x|}}{\sqrt{|x|}}\left(\frac{\partial e^{-ik\hat{x}\cdot y}}{\partial\nu(y)}+O\left(\frac{1}{|x|}\right)\right) \quad \text{as } |x|\to\infty.$$

Inserting these two expressions into the Green's representation formula (2.47) yields

$$\begin{aligned}w(x) = &\frac{e^{ik|x|}}{\sqrt{|x|}}\frac{e^{i\pi/4}}{\sqrt{8k\pi}}\int_{\partial D}\left(w(y)\frac{\partial e^{-ik\hat{x}\cdot y}}{\partial\nu(y)}-\frac{\partial w}{\partial\nu}(y)e^{-ik\hat{x}\cdot y}\right)ds(y)\\ &+\frac{e^{i(k|x|+\pi/4)}}{\sqrt{8k\pi}}\int_{\partial D}\left(w(y)\,O\left(\frac{1}{|x|^{3/2}}\right)-\frac{\partial w}{\partial\nu}(y)\,O\left(\frac{1}{|x|^{3/2}}\right)\right)ds(y)\end{aligned}$$

as $|x|\to\infty$. Since w and $\partial w/\partial\nu$ are continuous on ∂D, they have maxima on ∂D. Hence,

$$w(x) = \frac{e^{ik|x|}}{\sqrt{|x|}}\left[\frac{e^{i\pi/4}}{\sqrt{8k\pi}}\int_{\partial D}\left(w(y)\frac{\partial e^{-ik\hat{x}\cdot y}}{\partial\nu(y)}-\frac{\partial w}{\partial\nu}(y)e^{-ik\hat{x}\cdot y}\right)ds(y)\right]+O\left(\frac{1}{|x|^{3/2}}\right)$$

as $|x|\to\infty$. □

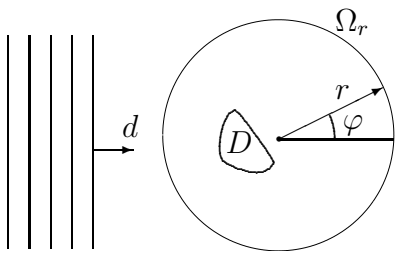

Figure 2.2: A time-harmonic incident plane wave with direction $d \in S^1$ of propagation (and wave number k), and a scattering obstacle D. The far field pattern F_D (together with r) determines the amplitude of the scattered field on the circle $\Omega_r := \{x \in \mathbb{R}^2 \ : \ |x| = r\}$ as r tends to infinity.

3. THE INVERSE PROBLEM AND THE FACTORIZATION METHOD

In this chapter we turn to the inverse scattering problem. There are in fact several possible inverse problems, but this thesis is only concerned with the following one: given far field patterns for all incident directions with a fixed wavenumber, find the shape of the sound-hard obstacle. This problem turns out to be nonlinear and ill-posed. The ill-posedness makes it a challenging problem especially from a numerical point of view. We begin this chapter with a brief review of the properties of this inverse problem. Then in the second section we study a relatively new method for solving inverse scattering problems. The method is known as factorization method.

3.1 The inverse problem

In addition to being inverse to a problem called direct problem, an inverse problem is (typically) ill-posed. According to Hadamard's classical definition a problem is well-posed if

(i) it has a solution,

(ii) the solution is unique, and

(iii) the solution is stable, i.e., it depends continuously on the data.

A problem that fails to satisfy at least one of these conditions is said to be ill-posed. The inverse scattering problem is ill-posed because it does not satisfy condition (iii) and in practical applications there may be problems with condition (i) also.

Let us now precisely formulate the inverse problem considered in this work:

The inverse problem: Given the far field pattern $F_D(\varphi; d, k)$ for all $\varphi, d \in S^1$ and fixed $k > 0$, determine the shape of the sound-hard obstacle D.

The rest of this section is devoted to considering this problem with respect to conditions (i)–(iii).

Assuming that the given data represents far field patterns of some obstacle, there clearly exists a solution. However, real-world measurements as well as numerical computations always contain errors, and hence it may happen that the given measurement data does not represent far field patterns, in which case the existence condition (i) is violated.

There are many uniqueness results for inverse scattering problems. The following theorem guarantees existence of a unique solution to our inverse problem.

Theorem 3.1.1. *Let D_1 and D_2 be two sound-hard scatterers whose far field patterns coincide for all incident directions and a fixed wave number. Then $D_1 = D_2$.*

Proof. See [12, Theorem 3.1.1]. □

This result verifies, at least in theory, that the knowledge of the far field patterns for all incident plane waves with a fixed wave number suffices to determine the obstacle uniquely, and in this sense the inverse problem is a reasonable problem from practical point of view.

Finally we consider the stability condition (iii). The inverse scattering problem begins from the knowledge of the far field patterns. To see the ill-posedness of the inverse problem we have to consider the mapping $w^s \mapsto F_D$ from the scattered field w^s to the far field pattern F_D defined by (2.53). This is due to the fact that the aim in the inverse problem is, in a sense, to recover the scattered field from the knowledge of the far field patterns: reconstructing the obstacle is equivalent to determining the zeros of the normal derivative $\partial w/\partial \nu$ of total field $w = w^i + w^s$ where the incident field w^i is known.

To rigorously verify the ill-posedness of the inverse problem we could use function series representations for scattered fields and for far field patterns or exploit functional analytic results for compact operators. Here we just state that the ill-posedness is caused by the smoothing effect of the integration in (2.53).

3.2 The factorization method

The factorization method is a relatively new method for solving shape identification problems related to inverse problems such as inverse scattering problems and electrical impedance tomography. It was developed by Andreas Kirsch and Natalia Grinberg. Detailed information and analysis, as well as references to the original publications, can be found in their recent monograph [9]. Here we just briefly outline the derivation of the method.

The factorization method (and its name) is based on a factorization of the far field operator $F : L^2(S^1) \to L^2(S^1)$ defined by

$$(Fg)(\varphi) = \int_{S^1} F_D(\varphi; d, k) g(d) ds(d), \quad \varphi \in S^1.$$

Notice that this operator contains all the information given in the far field patterns. The operator F is compact and has a factorization of the form

$$F = GTG^*,$$

where G and G^* are compact operators and T is an isomorphism between appropriate spaces. The fundamental result is that a point $z \in \mathbb{R}^2$ belongs to the obstacle D if and only if the function $\phi_z \in L^2(S^1)$, given by

$$\phi_z(\varphi) = e^{-ik\varphi\cdot z},$$

belongs to the range of G. This result is not very useful from computational point of view; however, a computationally attractive formulation can be achieved as follows. In the case of sound-hard obstacles (Neumann boundary conditions) the far field operator F can be shown to be normal, that is,

$$F^*F = FF^*,$$

where the operator F^* is the L^2-adjoint of F. Hence, from the spectral theory of normal operators we know that F can be represented as

$$Fg = \sum_{j=1}^{\infty} \lambda_j (g, \psi_j)\psi_j,$$

where $(\cdot,\cdot)$ denotes the L^2 inner product, and $\lambda_j \in \mathbb{C}$, $j = 1, 2, \ldots$ are the eigenvalues of F with the corresponding eigenfunctions ψ_j, $j = 1, 2, \ldots$. Moreover, it can be shown that the ranges of operators G and $(F^*F)^{1/4}$ coincide, where

$$(F^*F)^{1/4} g = \sum_{j=1}^{\infty} \sqrt{|\lambda_j|}(g, \psi_j)\psi_j.$$

Thus $z \in \mathbb{R}^2$ belongs to D if and only if there exists $g \in L^2(S^1)$ such that

$$(F^*F)^{1/4} g = \phi_z. \tag{3.1}$$

Writing $\phi_z = \sum_{j=1}^{\infty} (\phi_z, \psi_j)\psi_j$ and applying Picard's criterion we conclude that (3.1) is solvable if and only if

$$\sum_{j=1}^{\infty} \frac{|(\phi_z, \psi_j)|^2}{|\lambda_j|} \tag{3.2}$$

converges. The main result can now be formulated as follows.

Theorem 3.2.1. *Assume that k^2 is not a Neumann eigenvalue of $-\Delta$ in D, i.e., there exists no nontrivial solution $w \in C^2(D) \cap C^1(\overline{D})$ to the Helmholtz equation such that $\partial w/\partial \nu = 0$ on ∂D. Then $z \in \mathbb{R}^2$ belongs to D if and only if* (3.2) *converges,*

that is,

$$W(z) := \left(\sum_{j=1}^{\infty} \frac{|(\phi_z, \psi_j)|^2}{|\lambda_j|} \right)^{-1} > 0. \tag{3.3}$$

4. COMPUTATIONAL METHODS

We begin this chapter by developing a computational method for solving direct scattering problems including the determination of far field pattern. After that in the last section we create a numerical implementation of the factorization method. These computational methods will be illustrated with several numerical examples in the following chapter.

Finally a note on the mathematical notation. In this chapter we identify a point $(x_1, x_2) \in \mathbb{R}^2$ with the complex number $x_1 + ix_2$.

4.1 Direct problem

We consider the solution of the exterior Neumann problem

$$\begin{aligned} \Delta w + k^2 w &= 0 \quad \text{in } \mathbb{R}^2 \setminus \overline{D}, \\ \frac{\partial w}{\partial \nu} &= g \quad \text{on } \partial D, \\ \lim_{r\to\infty} \sqrt{r}\left(\frac{\partial w}{\partial r} - ikw\right) &= 0, \quad r = |x|, \end{aligned} \tag{4.1}$$

where D is assumed to have a piecewise C^1-smooth boundary ∂D and the function g is defined by

$$g(x) = -\frac{\partial}{\partial \nu} e^{ikx\cdot d}.$$

As shown in Chapter 2, the solution of this problem can be sought in the form of a single-layer potential representation

$$w(x) = \int_{\partial D} \Phi(x-y) f(y) ds(y), \quad x \in \mathbb{R}^2 \setminus \overline{D}, \tag{4.2}$$

where the continuous density $f \in C(\partial D)$ is a solution (not necessarily unique) of the integral equation

$$\left(\frac{1}{2} I - A\right) f = -g. \tag{4.3}$$

Here I is the identity operator and $A : C(\partial D) \to C(\partial D)$ is given by

$$(Af)(x) = \int_{\partial D} \frac{\partial \Phi(x-y)}{\partial \nu(x)} f(y) ds(y), \quad x \in \partial D.$$

In other words we have to first find a density f such that (4.3) is satisfied. Therefore, we begin by introducing a numerical method for solving (4.3).

We choose a 1-periodic piecewise C^1-smooth parametrization of the boundary curve ∂D as $x(t) = (x_1(t), x_2(t)),\ t \in [-1/2, 1/2]$. Denoting $f(t) = f(x(t))$ and $g(t) = g(x(t))$ equation (4.3) is equivalent to

$$\frac{1}{2}f(t) - (Af)(t) = -g(t), \tag{4.4}$$

where the integral operator A can be written in the following form using (2.32) and the chain rule:

$$\begin{aligned}(Af)(t) &= \frac{i}{4}\int_{-1/2}^{1/2} \frac{\partial H_0^{(1)}}{\partial \nu(x(t))} f(s)|x'(s)|ds \\ &= -\frac{ik}{4}\int_{-1/2}^{1/2} H_1^{(1)}(k|x(t)-x(s)|)\frac{\nu(x(t))\cdot(x(t)-x(s))}{|x(t)-x(s)|}f(s)|x'(s)|ds.\end{aligned}$$

To compute the integral in this expression we discretize the interval $[-1/2, 1/2]$ by choosing some $N \in \mathbb{N}$ and setting

$$s_j = jh, \quad j = -\frac{N}{2}, -\frac{N}{2}+1, \ldots, \frac{N}{2}-1, \quad h = \frac{1}{N}.$$

Then the integral can be approximated by the following sum:

$$h\sum_{j=-N/2}^{N/2-1} H_1^{(1)}(k|x(t)-x(s_j)|)\frac{\nu(x(t))\cdot(x(t)-x(s_j))}{|x(t)-x(s_j)|}f(s_j)|x'(s_j)|. \tag{4.5}$$

It is worth emphasizing that for $t = s_j$ there is a problem with the singularity of $H_1^{(1)}(z)$ at $z = 0$. We overcome this problem by omitting the corresponding term in the sum. Because of the weakly integrable nature of the singularity, the error caused by the omission becomes arbitrarily small as N grows.

Now that we have an approximate numerical implementation of the operator A, we can use some iterative solver (e.g. GMRES) to solve the Fredholm equation (4.4).

Having solved the density f we can approximately compute the actual solution (4.2) at any point $z \in \mathbb{R}^2 \setminus \overline{D}$ using the following expression:

$$h\frac{i}{4}\sum_{j=-N/2}^{N/2-1} H_0^{(1)}(k|z-x(s_j)|)f(s_j)|x'(s_j)|.$$

Finally, we consider the computation of the far field pattern F_D. This could be done using (2.53) but there is a more efficient way that does not require the solution w of the exterior Neumann problem, as shown in the following. Combining equations

(2.52) and (4.2), and using the asymptotic form (2.54) we obtain

$$\begin{aligned}\frac{e^{ikr}}{\sqrt{r}}F_D(\varphi;d,k) &= \int_{\partial D}\Phi(r\varphi-y)f(y)ds(y)+O\left(\frac{1}{r^{3/2}}\right)\\ &= \frac{e^{i\pi/4}}{\sqrt{8k\pi}}\frac{e^{ikr}}{\sqrt{r}}\int_{\partial D}e^{-ik\varphi\cdot y}f(y)ds(y)+O\left(\frac{1}{r^{3/2}}\right), \quad r\to\infty\end{aligned}$$

and hence the far field pattern F_D can be approximated as follows:

$$F_D(\varphi;d,k)\approx\frac{e^{i\pi/4}}{\sqrt{8k\pi}}\int_{\partial D}e^{-ik\varphi\cdot y}f(y)ds(y). \tag{4.6}$$

Approximating the integral over ∂D in the same manner as above, we can now compute the far field pattern using the expression

$$h\frac{e^{i\pi/4}}{\sqrt{8k\pi}}\sum_{j=-N/2}^{N/2-1}e^{-ik\varphi\cdot x(s_j)}f(s_j)|x'(s_j)|$$

for any $\varphi\in S^1$. To compute the far field patterns we choose $n\in\mathbb{N}$ evenly distributed directions $\varphi_1,\ldots,\varphi_n$, where $\varphi_j=e^{i2j\pi/n}$.

4.2 The factorization method

Next we consider a numerical implementation of the factorization method. The implementation is based on the indicator function W defined in (3.3). We notice that computing values of W requires the knowledge of the eigenvalues and eigenfunctions of the far field operator F. Hence we start from the computation of this eigensystem using singular value decomposition.

Assume that the far field pattern $F_D(\varphi;d,k)$ is given at points

$$\varphi_j=d_j=e^{is_j}\text{ for }j=1,\ldots,n,$$

where $s_j=2j\pi/n$. Then the integral operator F,

$$(Fg)(\varphi)=\int_{S^1}F_D(\varphi;d,k)g(d)ds(d),$$

can be approximately computed at points $\varphi_1,\ldots,\varphi_n$ as

$$(Fg)(\varphi_l)\approx\sum_{j=1}^{n}F_D(\varphi_l;d_j,k)g(d_j),$$

and hence the operator F can be represented as the matrix $A\in\mathbb{C}^{n\times n}$ with elements $A_{lj}=F_D(\varphi_l;d_j,k)$. To get an approximation for the eigenvalues and eigenvectors

of F we compute the singular value decomposition

$$A = UDV^*,$$

where D is a diagonal matrix with the singular values $\sigma_1, \ldots, \sigma_n > 0$ of A on its diagonal. We approximate the eigenvalues $|\lambda_j|$ in (3.3) with the singular values σ_j and the corresponding eigenfunctions ψ_j with the column vectors $V_j = [v_{1j}, \ldots, v_{nj}]^T$ of matrix V. The indicator function W given by (3.3) can then be approximately computed as follows:

$$W(z) \approx \left(\sum_{j=1}^{n} \frac{\left| \sum_{l=1}^{n} \exp(-ik\varphi_l \cdot z) v_{lj} \right|^2}{\sigma_j} \right)^{-1}. \tag{4.7}$$

The value of W is smaller for points $z \in D$ than for $z \notin D$. Hence we can approximately reconstruct the obstacle by choosing some $R > 0$ such that any $z \in \mathbb{R}^2$ with $W(z) \geq R$ is considered to lie in D whereas $W(z) < R$ implies $z \notin D$.

5. NUMERICAL RESULTS

This chapter illustrates with numerical examples the scattering problems and computational methods presented in the preceding chapters. The first section presents solutions to several direct problems, i.e., the scattered fields and their far field patterns for several different obstacles and incident fields. The results of the corresponding inverse problems solved with the factorization method are presented in the second section.

The following note on the wave number is worth emphasizing. As pointed out in [5, Section 1.1], the mathematical methods for solving scattering problems are dependent on the wave number k. More precisely, the methods presented in this thesis are physically reasonable only in the so-called resonance region in which $ka \lesssim 1$, where a is the diameter of the scattering obstacle. This fact was taken into account when choosing the wave numbers for the numerical examples presented in this chapter.

In addition to visual illustrations some numerical values provide useful information about the results. In this chapter we measure the difference between two matrices A and B by

$$\text{diff} := \frac{\|A - B\|_F}{(1/2)\big(\|A\|_F + \|B\|_F\big)}, \tag{5.1}$$

where $\|\cdot\|_F$ denotes the Frobenius norm. This value is used to measure differences between two far field patterns and between two reconstructions of obstacles.

5.1 Direct problem

The numerical examples were chosen such that they illustrate

(1) a difference between scattered fields and far field patterns for two somewhat similar obstacles,

(2) that the mapping from the obstacle to the far field pattern is nonlinear[1], and

(3) scattered fields and their far field patterns for obstacles with corners.

[1]The nonlinearity here is somewhat unclear concept, since we have no linear structure in the set of obstacles $D \subset \mathbb{R}^2$, but the idea of the example hopefully becomes clear when seeing the results.

We remark that (2) is an interesting fact with respect to the corresponding inverse problem, since it implies that the inverse problem is not merely ill-posed but also nonlinear. In cases (1) and (2) the following are presented:

(i) the scattered field caused by a plane wave of the form $e^{ikx\cdot d}$, where $d = (1, 0)$, and

(ii) the far field pattern

with three different wave numbers k. In all the examples the number of discretization points for the boundary of the obstacle is $N = 256$ and for the incident and observation directions in far field patterns $n = 256$.

The far field patterns are plotted such that the horizontal and vertical axes correspond to the observation direction d and to the incident direction φ, respectively. Both axes range from 0 to 2π.

5.1.1 Comparison between two obstacles

Consider the two obstacles shown in Figure 5.1 with their scattered fields. Notice the similarities and differences between these obstacles. The corresponding far field patterns are shown in Figure 5.2.

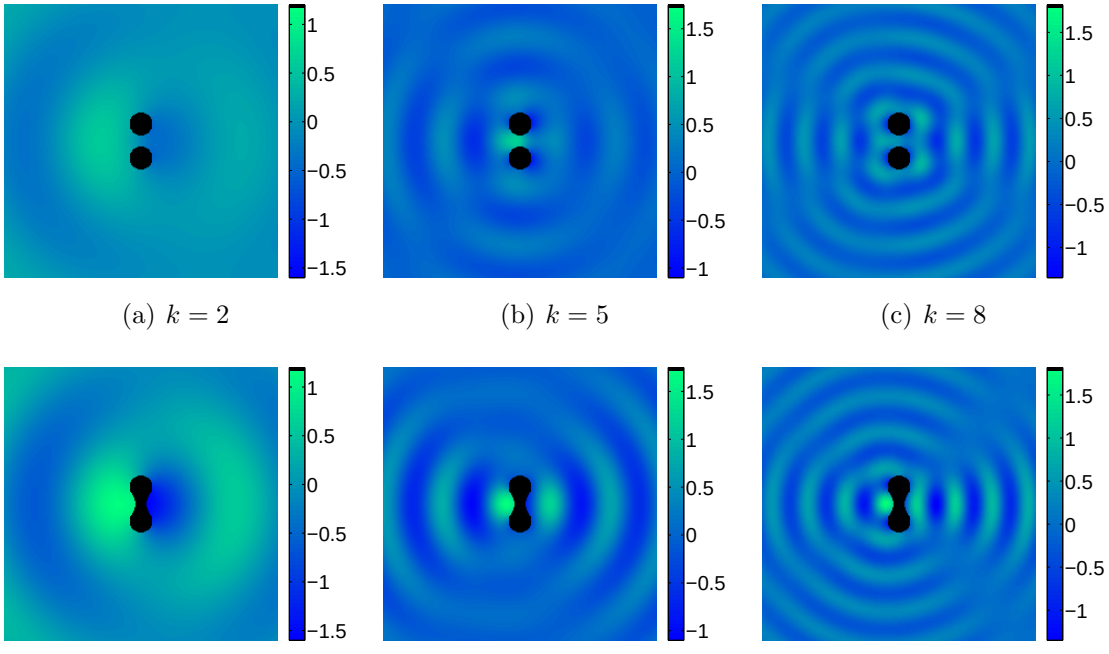

(a) $k = 2$ (b) $k = 5$ (c) $k = 8$

(d) $k = 2$ (e) $k = 5$ (f) $k = 8$

Figure 5.1: Scattered fields with different wave numbers k for two somewhat similar obstacles. The black areas depict the obstacles. The diameter of both obstacles is 5/8.

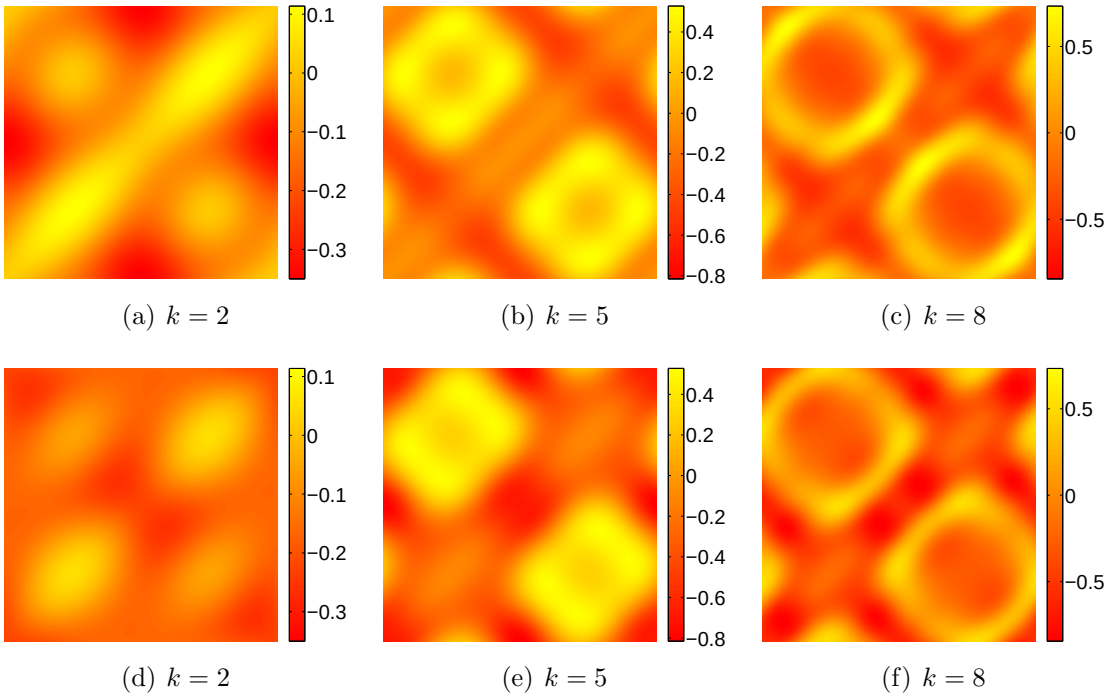

(a) $k = 2$ (b) $k = 5$ (c) $k = 8$

(d) $k = 2$ (e) $k = 5$ (f) $k = 8$

Figure 5.2: Far field patterns for the two obstacles shown in Figure 5.1. The relative differences (diff) defined by (5.1) are 74% between (a) and (d), 65% between (b) and (e), and 66% between (c) and (f).

5.1.2 Illustration of nonlinearity

The aim of this example is to illustrate the nonlinearity of the mapping from the obstacle to the far field pattern. Consider the obstacles 1, 2 and 3 in Figure 5.3. The obstacle 3 can be viewed, in a sense, as the sum of obstacles 1 and 2. However, as can be seen from Figure 5.4, the sum of the far field patterns of obstacles 1 and 2 is *not* equal to the far field pattern of obstacle 3.

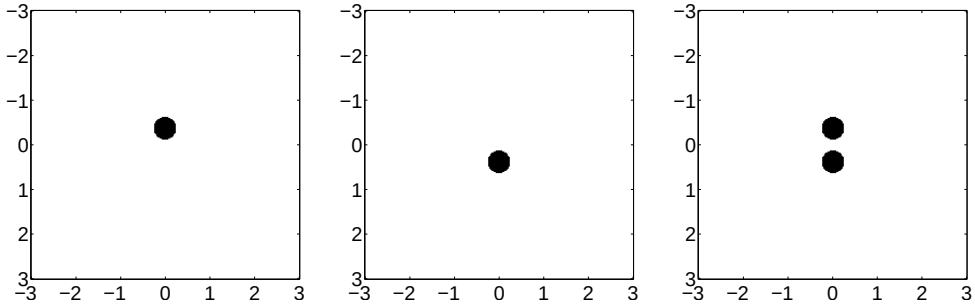

(a) Obstacle 1 (b) Obstacle 2 (c) Obstacle 3

Figure 5.3: Obstacles 1 and 2 together form obstacle 3.

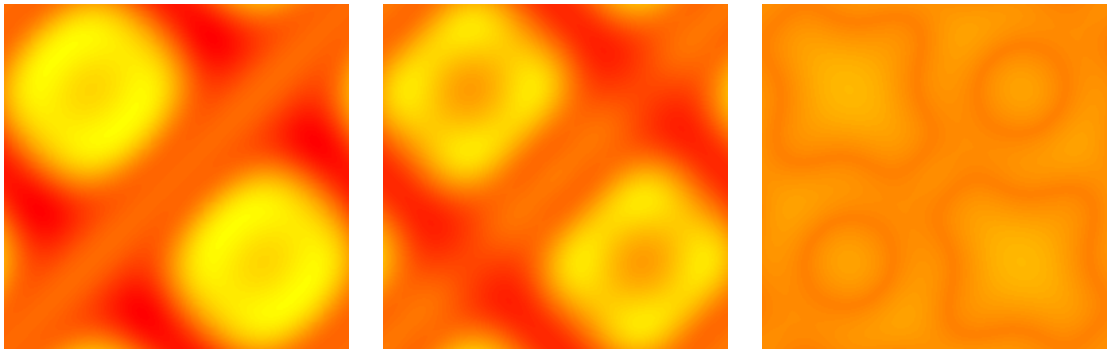

(a) The sum of the far field patterns of obstacles 1 and 2

(b) The far field pattern of obstacle 3

(c) The difference of the far field patterns (a) and (b)

Figure 5.4: The difference of the two far field patterns was computed as in Figure 5.2. The difference was computed by first subtracting the two far field patterns (i.e., matrices) and then taking the componentwise absolute value of the difference matrix. The wave number $k = 5$. Color scale ranges from -0.65 (red) to 0.65 (yellow).

5.1.3 Obstacles with corners

Despite the fact that most of the theoretical results in scattering theory have been derived for obstacles with C^2-smooth boundaries, it presents no difficulties to compute the scattered fields and their far field patterns for obstacles having piecewise C^1-smooth boundaries only. In terms of real-world obstacles it is not even reasonable to assume that some obstacle would have a C^2-smooth boundary. Hence the theory requiring C^2-smooth boundaries can be seen as a model which approximates the reality accurately enough to be a valuable tool in analyzing and predicting natural phenomena. Next we consider obstacles with piecewise C^1-smooth boundaries, that is, obstacles with corners.

To illustrate the effect of a corner in the scattering obstacle, we present scattered fields and their far field patterns for two obstacles with corners and for two otherwise similar obstacles but with the corner "smoothened", see Figures 5.5 and 5.7. The far field patterns and their differences are shown in Figures 5.6 and 5.8. The differences of two far field patterns, i.e. matrices, was computed by first subtracting the matrices and then taking the componentwise absolute value.

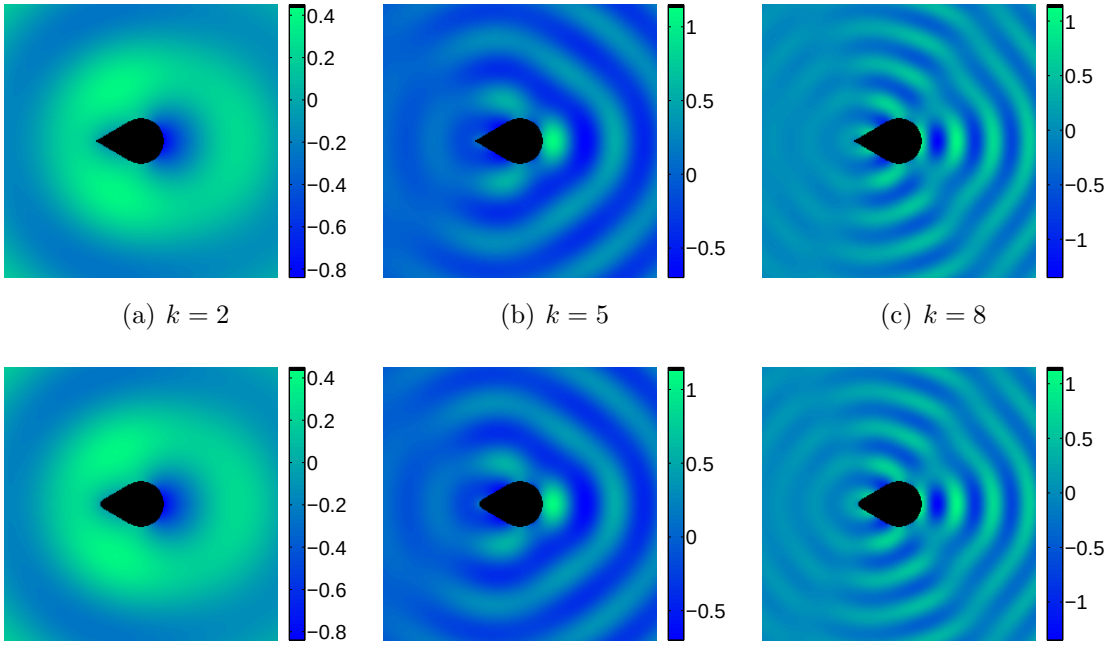

(a) $k = 2$ (b) $k = 5$ (c) $k = 8$

(d) $k = 2$ (e) $k = 5$ (f) $k = 8$

Figure 5.5: The scattered fields with different wave numbers k for an obstacle with a corner (upper row), and for the "smoothened" version of the same obstacle (lower row). The black areas depict the obstacles. The diameter of both obstacles is approximately 1.5.

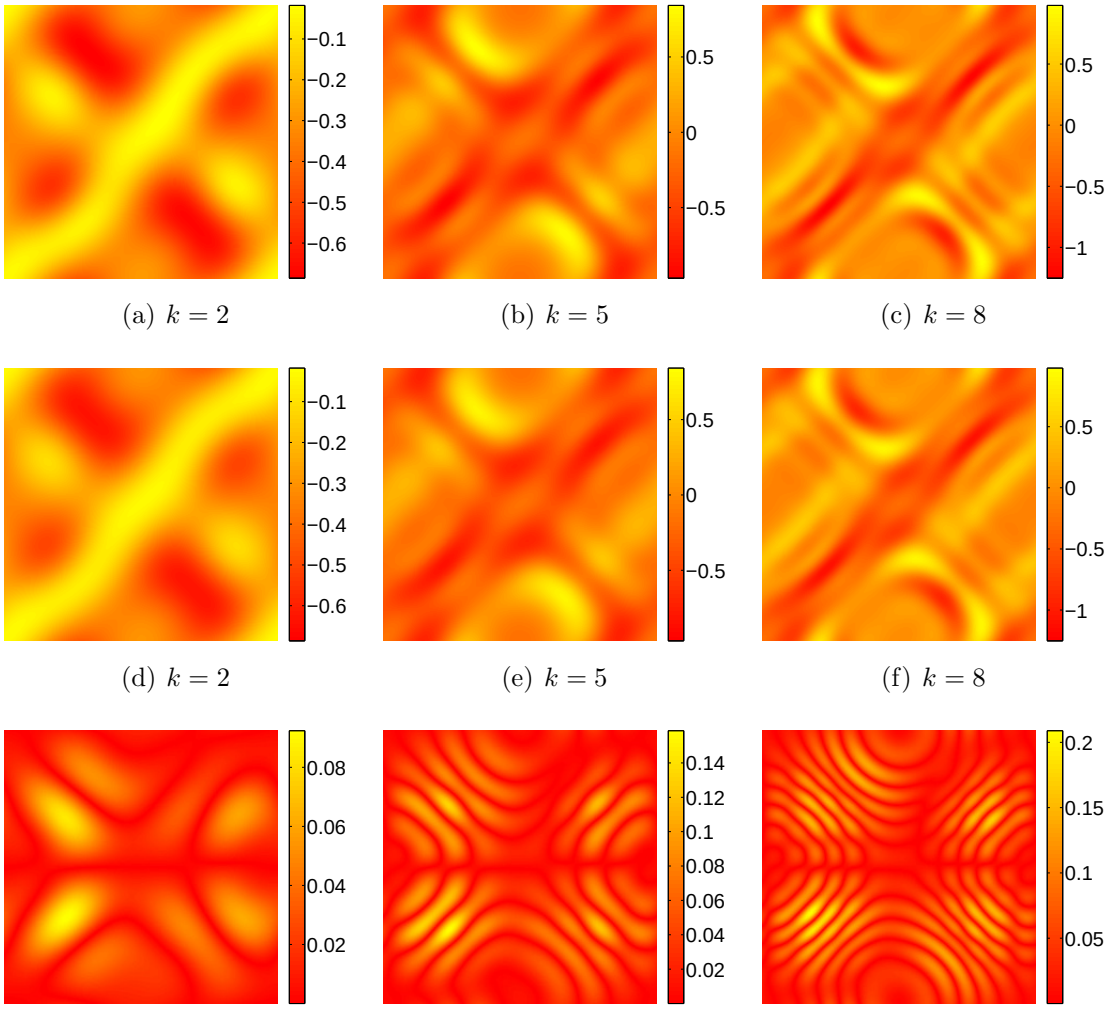

(a) $k = 2$ (b) $k = 5$ (c) $k = 8$

(d) $k = 2$ (e) $k = 5$ (f) $k = 8$

(g) $k = 2$, diff=8% (h) $k = 5$, diff=12% (i) $k = 8$, diff=15%

Figure 5.6: Far field patterns and their differences for the two obstacles shown in Figure 5.5: the far field patterns on the first row correspond to the obstacle on the upper row in Figure 5.5, and similarly the far field patterns on the second row correspond to the obstacle on the lower row in Figure 5.5. The last row shows the differences of the far field patterns on the first and second rows.

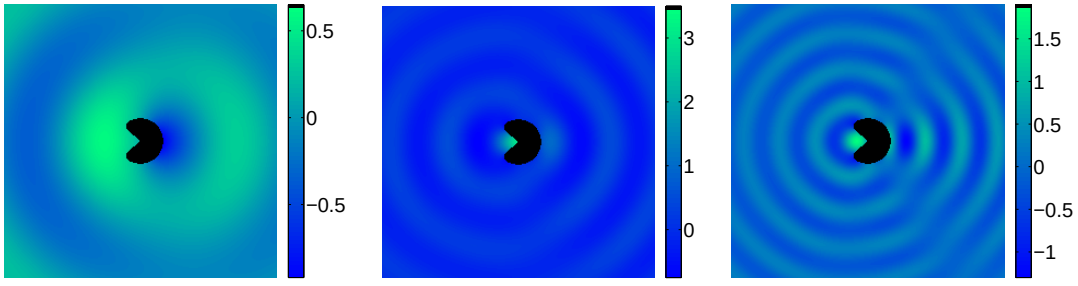

(a) $k = 2$ (b) $k = 5$ (c) $k = 8$

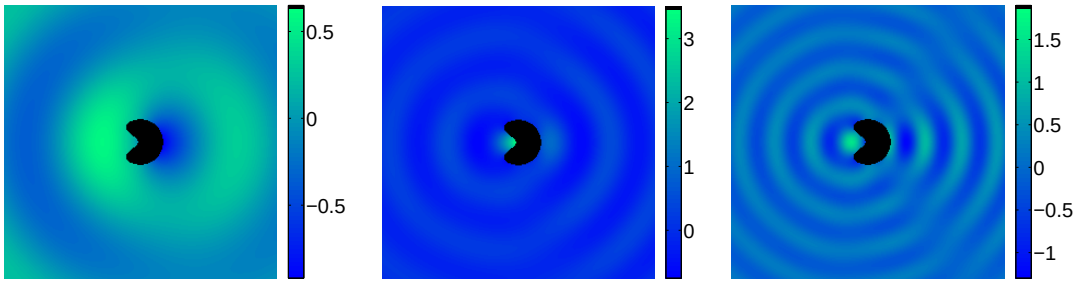

(d) $k = 2$ (e) $k = 5$ (f) $k = 8$

Figure 5.7: The scattered fields with different wave numbers k for an obstacle with a corner (upper row), and for the "smoothened" version of the same obstacle (lower row). The black areas depict the obstacles. The diameter of both obstacles is approximately 1.

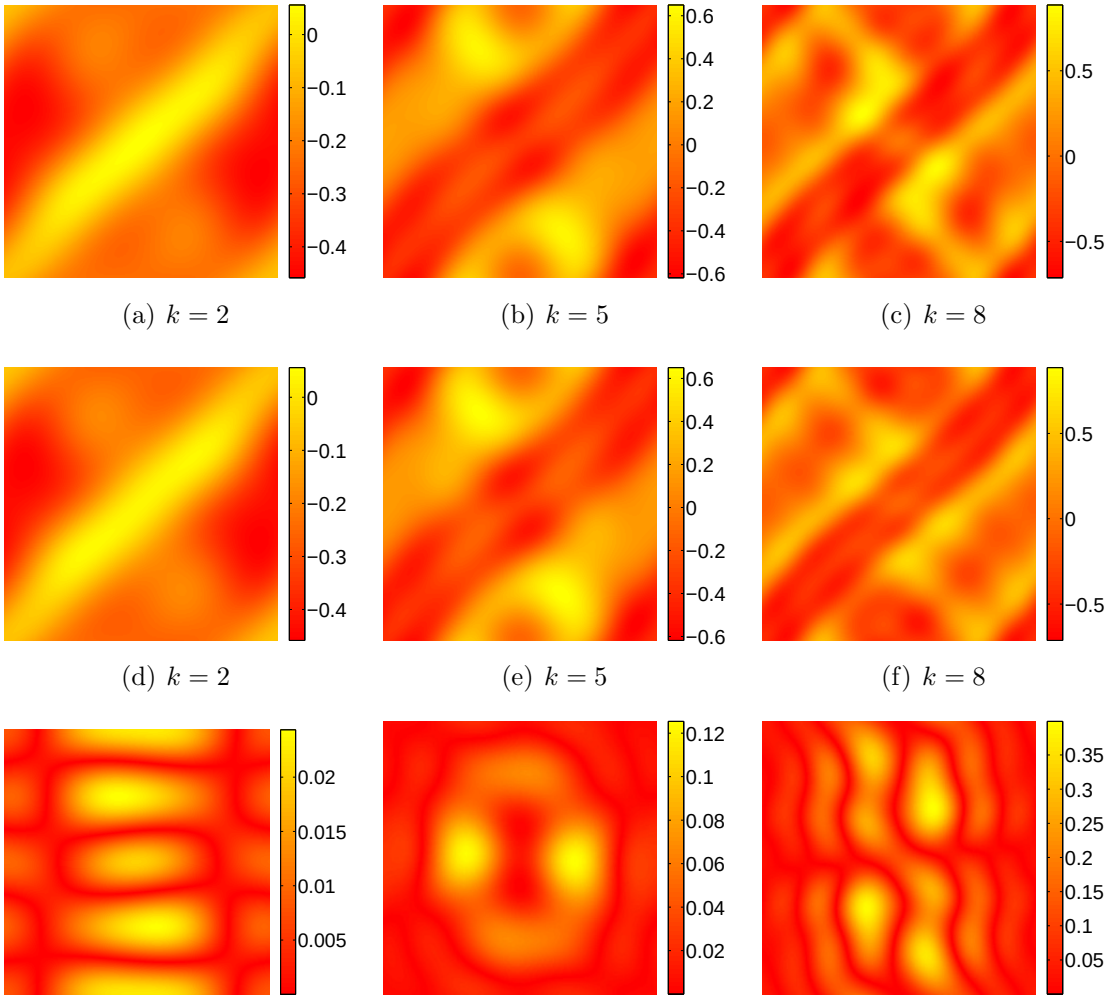

(a) $k = 2$ (b) $k = 5$ (c) $k = 8$

(d) $k = 2$ (e) $k = 5$ (f) $k = 8$

(g) $k = 2$, diff=4% (h) $k = 5$, diff=13% (i) $k = 8$, diff=39%

Figure 5.8: Far field patterns and their differences for the two obstacles shown in Figure 5.7. The representation is similar to Figure 5.6.

5.2 Inverse problem

Next we turn to the results obtained by applying the factorization method to the far field patterns (of the obstacles) presented in the preceding section. We present the reconstructions both from ideal noise-free data and from data with 1% white noise. The term reconstruction here refers in fact to the plot of the indicator function W computed using (4.7). In order to precisely answer to the problem "find the shape of the obstacle" we have to choose some number $R > 0$ such that $W(z) \geq R$ implies $z \in D$ and $W(z) < R$ implies $z \notin D$. However, the plots of the indicator function contain more information than the actual reconstructions and hence we present these plots and refer to them as reconstructions.

5.2.1 Reconstructions from ideal and noisy data

We begin with the reconstructions from ideal data and from data with 1% white noise added. The reconstructions of each obstacle are presented for a wave number that approximately produced the best reconstruction by visual inspection. To get insight into the effect of the choice of the wave number see the following section. The reconstructions with original obstacles are shown in Figures 5.9, 5.10 and 5.11.

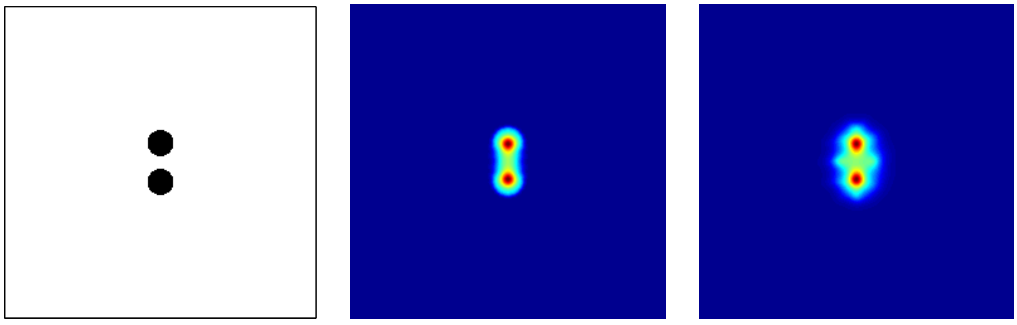

(a) The obstacle (b) Ideal data (c) Noisy data

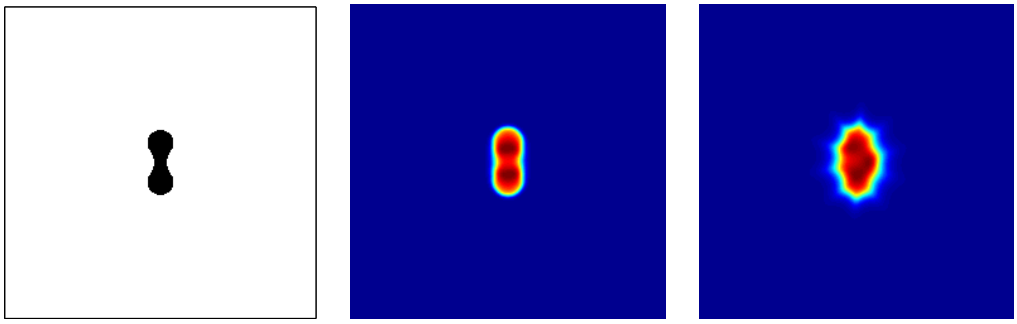

(d) The obstacle (e) Ideal data (f) Noisy data

Figure 5.9: Reconstructions from ideal and noisy data, and the original obstacles (left column). The noisy data was created by adding 1% white noise to the ideal data. The wave number for the obstacle on the upper row is $k = 6$, and for the obstacle on the lower row $k = 4$. The color scale ranges from 0 (dark blue) to 0.2 (dark red).

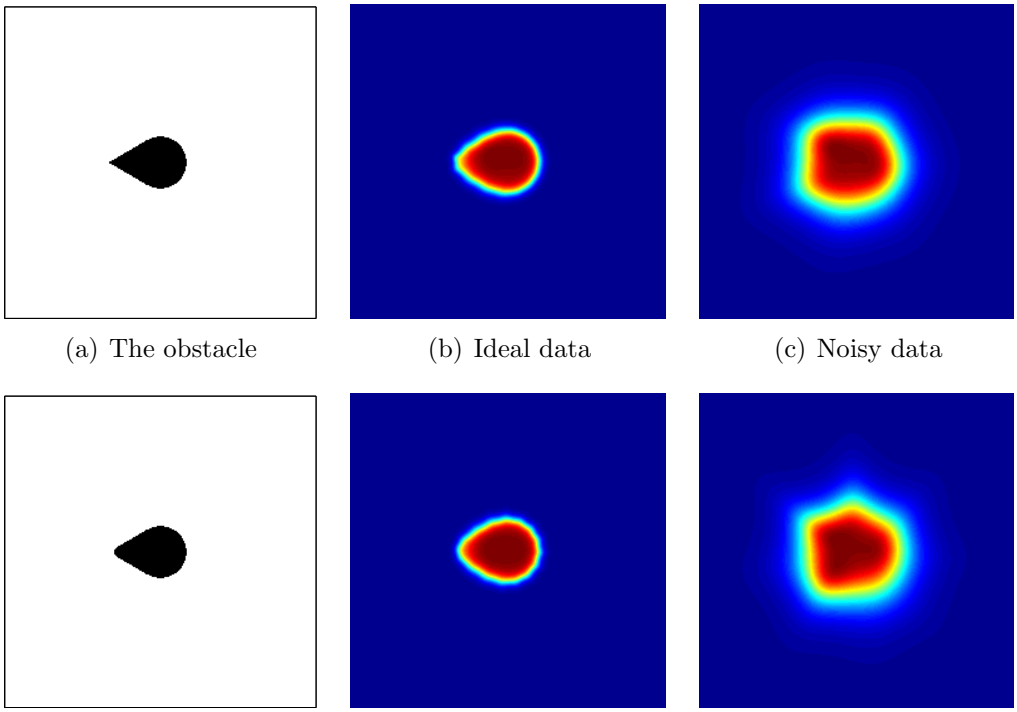

(a) The obstacle (b) Ideal data (c) Noisy data

(d) The obstacle (e) Ideal data (f) Noisy data

Figure 5.10: Reconstructions from ideal and noisy data, and the original obstacles (left column). The noisy data was created by adding 1% white noise to the ideal data. The obstacle on the first row has a corner that is smoothened in the obstacle on the lower row. The wave number for both obstacles is $k = 1$. The difference (diff) of the reconstructions (b) and (e) is 5%. The color scale ranges from 0 (dark blue) to 0.15 (dark red).

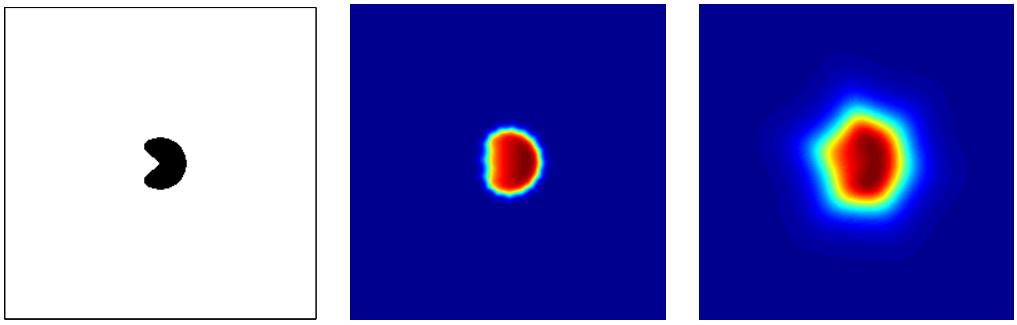

(a) The obstacle (b) Ideal data (c) Noisy data

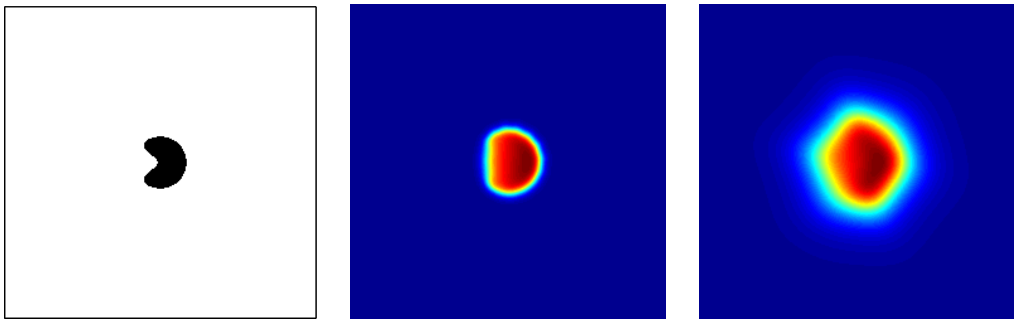

(d) The obstacle (e) Ideal data (f) Noisy data

Figure 5.11: Reconstructions from ideal and noisy data, and the original obstacles (left column). The noisy data was created by adding 1% white noise to the ideal data. The obstacle on the first row has a corner that is smoothened in the obstacle on the lower row. The wave number for both obstacles is $k = 1$. The difference (diff) of the reconstructions (b) and (e) is 3%. The color scale ranges from 0 (dark blue) to 0.11 (dark red).

5.2.2 Dependence on the wave number

To illustrate how the results of the factorization method depend on the choice of the wave number, we present reconstructions from ideal data for two obstacles with five different wave numbers. The reconstructions are shown in Figure 5.12.

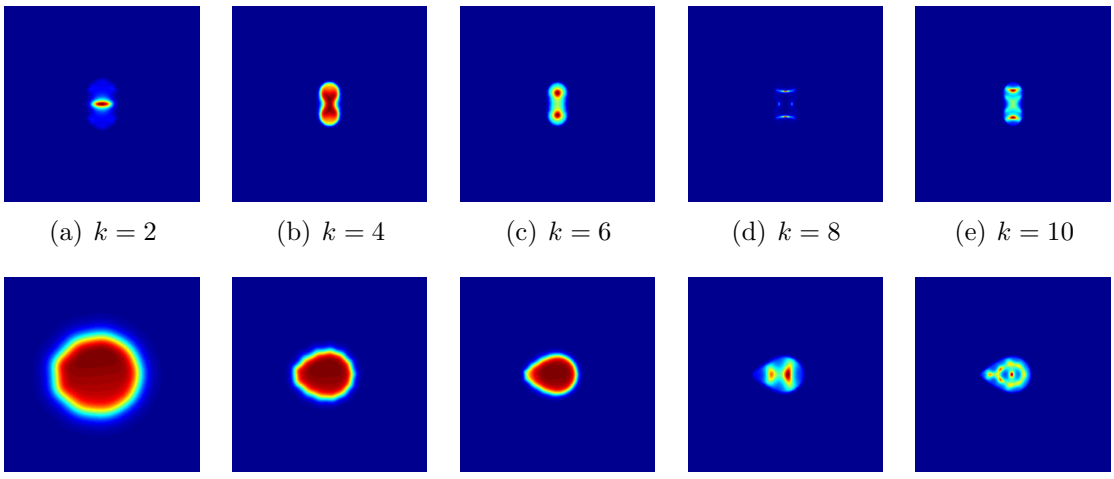

(a) $k = 2$ (b) $k = 4$ (c) $k = 6$ (d) $k = 8$ (e) $k = 10$

(f) $k = 0.1$ (g) $k = 0.5$ (h) $k = 1$ (i) $k = 5$ (j) $k = 10$

Figure 5.12: Reconstructions from ideal data for two obstacles with five different wave numbers k. The obstacles are the one on the upper row in Figure 5.9 and the one on the upper row in Figure 5.10. The color scale is *not* the same in all reconstructions but chosen individually for each plot.

6. CONCLUSION

The theory of direct scattering problems makes use of a large variety of mathematical tools such as real, complex and functional analysis, and the theory of boundary value problems of partial differential equations. Especially establishing the existence of a solution to the direct scattering problem by using the method of boundary integral equations is a lengthy process that requires technical regularity results for the single-layer potential as well as abstract results for compact operators.

There are certain differences between two- and three-dimensional scattering theory and most of them arise from the fact that the fundamental solution of the Helmholtz equation is different in two and three dimensions. The differences become apparent in analyzing the regularity properties of the single-layer potential as well as in the formulation of the Sommerfeld radiation condition and in the far field pattern. Most of the literature on scattering theory deals with the practically more interesting three-dimensional case but the two-dimensional scattering problem serves as useful test problem especially in terms of numerical experiments.

The solution of the exterior Neumann problem arising from the direct scattering problem can easily be computed numerically by solving a boundary integral equation and using the corresponding single-layer potential representation of the solution. The computational methods and their numerical results presented in this work apparently seem to be correct since the reconstructions computed with the factorization method from the numerical results of the direct problem are excellent.

As can be seen from the numerical results, the factorization method is a promising qualitative method for solving inverse scattering problems, i.e., it can be used not only to detect but also to find information about the obstacle such as the number of the separate components of the obstacle. It gives a sufficient and necessary condition for a point to belong in the scattering obstacle, and the condition is easily and simply computable. The major drawback of the factorization method is that it needs a large amount of data for the inversion. Moreover, there are still many important scattering problems for which the factorization method has not been established.

REFERENCES

[1] Abramowitz M and Stegun I A (1965), *Handbook of Mathematical Functions with Formulas, Graphs and Mathematical Tables*, Dover.

[2] Cakoni F and Colton D (2006), *Qualitative Methods in Inverse Scattering Theory*, Springer.

[3] Chadan K, Colton D, Päivärinta L and Rundell W (1997), *An Introduction to Inverse Scattering and Inverse Spectral Problems*, SIAM.

[4] Colton D and Kress R (1983), *Integral Equation Methods in Scattering Theory*, John Wiley & Sons.

[5] Colton D and Kress R (1998), *Inverse Acoustic and Electromagnetic Scattering Theory*, Springer.

[6] Fitzpatrick P M (2006), *Advanced Calculus*, Thomson Brooks/Cole.

[7] Ghosh Roy D N and Couchman L S (2002), *Inverse problems and inverse scattering of plane waves*, Academic Press.

[8] Kirsch A (1996), *An Introduction to the Mathematical Theory of Inverse Problems*, Springer.

[9] Kirsch A and Grinberg N I (2008), *The Factorization Method for Inverse Problems*, Oxford University Press.

[10] Kirsch A and Kress R (1993), *Uniqueness in inverse obstacle scattering*, Inverse Problems **9**, 285-299.

[11] Lebedev N N (1972), *Special Functions & Their Applications*, Dover.

[12] Potthast R (2001), *Point sources and multipoles in inverse scattering theory*, Chapman & Hall/CRC.

[13] Saranen J and Vainikko G (2002), *Periodic Integral and Pseudodifferential Equations with Numerical Approximation*, Springer.

[14] Sommerfeld A (1912), *Die Greensche Funktion der Schwingungsgleichung*, Jahresber. Deutsch. Math. Verein. **21**, 309-353.